

---

# Regularization can make diffusion models more efficient

---

Mahsa Taheri<sup>1</sup> Johannes Lederer<sup>1</sup>

## Abstract

Diffusion models are one of the key architectures of generative AI. Their main drawback, however, is the computational costs. This study indicates that the concept of sparsity, well known especially in statistics, can provide a pathway to more efficient diffusion pipelines. Our mathematical guarantees prove that sparsity can reduce the input dimension’s influence on the computational complexity to that of a much smaller intrinsic dimension of the data. Our empirical findings confirm that inducing sparsity can indeed lead to better samples at a lower cost.

## 1. Introduction

Diffusion models are probabilistic generative models that generate new data similar to those they are trained on (Song and Ermon, 2019; Ho et al., 2020; Song et al., 2021b). These models have recently gained significant attention due to their impressive performance at image generation, video synthesis, text-to-image translation, and molecular design (Dhariwal and Nichol, 2021; Ho et al., 2022; Ramesh et al., 2022; Xu et al., 2022).

A diffusion generative model is based on two stochastic processes:

1. A forward process  $\mathbf{x}_0 \rightarrow \mathbf{x}_1 \rightarrow \dots \rightarrow \mathbf{x}_T$  that starts from a sample  $\mathbf{x}_0 \in \mathbb{R}^d$  from a target data distribution  $q_0$  ( $\mathbf{x}_0 \sim q_0$ ) and then diffuses this sample in  $T$  steps into pure noise  $\mathbf{x}_T \in \mathbb{R}^d$  ( $\mathbf{x}_T \sim \mathcal{N}(\mathbf{0}_d, \mathbb{I}_d)$ ).
2. A reverse process  $\mathbf{y}_T \rightarrow \mathbf{y}_{T-1} \rightarrow \dots \rightarrow \mathbf{y}_0$  that starts from pure noise  $\mathbf{y}_T \in \mathbb{R}^d$  ( $\mathbf{y}_T \sim \mathcal{N}(\mathbf{0}_d, \mathbb{I}_d)$ ) and then converts this noise in  $T$  steps into a new sample  $\mathbf{y}_0 \in \mathbb{R}^d$  ( $\mathbf{y}_0 \sim p_0$ ) that is similar in distribution to the target sample  $\mathbf{x}_0 \in \mathbb{R}^d$ .

Making the data noisy is easy. Therefore, fitting a good reverse process is the key to successful diffusion modeling.

---

<sup>1</sup>Department of Mathematics, Computer Science, and Natural Sciences, Hamburg University, Germany. Correspondence to: Mahsa Taheri <mahsa.taheri@uni-hamburg.de>.

The three predominant formulations of diffusion models are denoising diffusion probabilistic models (DDPM) (Ho et al., 2020), score-based generative models (SGM) (Song and Ermon, 2019), and score-based stochastic differential equations (SDE) (Song et al., 2021b;a). DDPM include two Markov chains: a forward process that transforms data into noise, and a reverse process that recovers the data from the noise. The objective is to train a function (usually a deep neural network) for denoising the data over time. Sample generation then takes random Gaussian noise through the trained denoising function. SGM, which is the setting adopted in this paper, also perturb data with a sequence of Gaussian noise but then try to estimate the score functions, the gradient of the log probability density, for the noisy data. Sampling combines the trained scores with score-based sampling approaches like Langevin dynamics. While DDPM and SGM focus on discrete time steps, Score SDEs consider infinitely many time steps or unbounded noise levels. In Score SDEs, the desired score functions are solutions of stochastic differential equations. Once the desired score functions are trained, sampling can be reached using stochastic or ordinary differential equations.

Much research efforts are geared toward non-asymptotic rates of convergence, particularly in the number of steps  $T$  needed to achieve a desired level of reconstruction accuracy. Typical measures of accuracy are Kullback–Leibler divergence, total variation, and Wasserstein distance between the true distribution  $\mathbb{Q}_0$  and the approximated counterpart  $P_0$ . For example, one tries to ensure  $\text{TV}(\mathbb{Q}_0, P_0) \leq \tau$  for a fixed error level  $\tau \in (0, \infty)$ , where  $\text{TV}(\mathbb{Q}_0, P_0) := \sup_{A \subset \mathbb{R}^d} |\mathbb{Q}_0(A) - P_0(A)|$  is called the total variation (van de Geer, 2000). The many very recent papers on this topic highlight the large interest in this topic (Block et al., 2020; De Bortoli et al., 2021; De Bortoli, 2022; Lee et al., 2022; Chen et al., 2023c;a; Li et al., 2024b; Chen et al., 2023e; Liang et al., 2024). Results like Block et al. (2020, Theorem 13) provide rates of convergence for diffusion models in terms of Wasserstein distance employing Langevin dynamics, but they suffer from the curse of dimensionality in that the rates depend exponentially on the dimensions of the data  $d$ , that is, the number of input features. Improved convergence rates in terms of  $d$  are proposed by Chen et al. (2023c); Li et al. (2024b), showing polynomial growth in  $d$ . Recently Liang et al. (2024) proposed a new

Hessian-based accelerated sampler for the stochastic diffusion processes. They achieve accelerated rate for the total variation convergence for DDPMs of the order  $d^{1.5}/\tau$  for any target distributions having finite variance and assuming a uniform bound over the accuracy of the estimated score function (see our Section 5 for an overview of recent works). While these results are a major step forward, they involve a strong dependence the dimensionality of the data, which is problematic as images, text, and so forth a typically high dimensional. The key question is whether improving these rates with respect to  $d$  is possible at all.

**Contribution** This paper aims to enhance the efficiency of diffusion models through the incorporation of regularization techniques commonly used in high-dimensional statistics (Lederer, 2022).

The contributions of this work are as follows:

- We theoretically demonstrate that  $\ell_1$ -regularization can enhance the convergence rates of diffusion models to the order of  $s^2/\tau$ , where  $s \ll d$ , compared to the standard order of  $d^2/\tau$  (Theorem 3.5).
- We validate our theoretical findings through simulations on image datasets (Section 6).
- We additionally demonstrate that  $\ell_1$ -regularization can make sampling more balanced and avoid oversmoothing (Section 6.3).

Thus, our research is a step forward in the whole field’s journey of improving our understanding of diffusion models and of making diffusion modeling more efficient.

**Paper outline** Section 2 introduces score matching and the discrete-time diffusion process. Section 3 presents our proposed estimator along with the main results (Theorem 3.5). Section 4 includes some technical results and Section 5 provides an overview of related work. We support our theoretical findings with numerical observations over image datasets in Section 6. Finally, we conclude the paper in Section 7. Additional simulations, technical results, and detailed proofs are provided in the Appendix.

## 2. Preliminaries of score matching and discrete-time diffusion process

In this section, we provide a brief introduction to score matching and discrete-time diffusion process.

**Notations** For a vector  $\mathbf{z} \in \mathbb{R}^d$ , we use the notation  $\|\mathbf{z}\|_1 := \sum_{i=1}^d |z_i|$ ,  $\|\mathbf{z}\|^2 := \sum_{i=1}^d (z_i)^2$ ,  $\|\mathbf{z}\|_\infty := \sup_{i \in \{1, \dots, d\}} |z_i|$ , and  $\|\mathbf{z}\|_0 := \sum_{i=1}^d \mathbf{1}(z_i \neq 0)$ .

### 2.1. Score matching

Assume a dataset  $\mathcal{D}_n := \{\mathbf{x}^1, \dots, \mathbf{x}^n\}$  of  $n$  training data samples  $\mathbf{x}^i \in \mathbb{R}^d$  with an unknown target distribution  $q_0$  ( $\mathbf{x}^i \sim q_0$  for  $i \in \{1, \dots, n\}$ ). The goal of probabilistic generative modeling is to use the dataset  $\mathcal{D}_n$  to learn a model that can sample from  $q_0$ . The score of a probability density  $q(\mathbf{x})$ , the gradient of the log-density with respect to  $\mathbf{x}$  denoted as  $\nabla_{\mathbf{x}} \log q(\mathbf{x})$ , are the key components for generating new samples from  $q$ . The score network  $\mathbf{s}_\Theta : \mathbb{R}^d \rightarrow \mathbb{R}^d$  is then a neural network parameterized by  $\Theta \in \mathcal{B}$ , which will be trained to approximate the unknown score  $\nabla_{\mathbf{x}} \log q_0(\mathbf{x})$ . The corresponding objective functions for learning scores in SGMs (Song and Ermon, 2019) is then based on Hyvärinen and Dayan (2005); Hyvärinen (2007)

$$\Theta^* \in \arg \min_{\Theta \in \mathcal{B}} \mathbb{E}_{q_0(\mathbf{x})} [\|\mathbf{s}_\Theta(\mathbf{x}) - \nabla_{\mathbf{x}} \log q_0(\mathbf{x})\|^2], \quad (1)$$

which yields the parameters of a neural network  $\mathbf{s}_{\Theta^*}(\mathbf{x})$  that approximates the unknown score function  $\nabla_{\mathbf{x}} \log q_0(\mathbf{x})$ . Of course, the objective function in (1) entails (i) an expectation over  $q_0$  and (ii) the true score  $\nabla_{\mathbf{x}} \log q_0(\mathbf{x})$ , which are both not accessible in practice. The expectation can readily be approximated by an average over the data samples  $\mathcal{D}_n$ ; replacing the score needs more care (Vincent, 2011; Song et al., 2020). We come back to this point later in Section 2.2 by representing a time dependent form of denoising score matching (Vincent, 2011). Once the score function is trained, there are various approaches to generate new samples from the target distribution  $q_0$  employing the approximated score. These include deterministic and stochastic samplers (see Li et al. (2024b) for an overview), Langevin dynamics among the most popular one (Song and Ermon, 2019).

### 2.2. Discrete-time diffusion process

Let’s  $\mathbf{x} \in \mathbb{R}^d$  be an initial data sample and  $\mathbf{x}_t \in \mathbb{R}^d$  for a discrete time step  $t \in \{1, \dots, T\}$  be the latent variable in the diffusion process. Let  $\mathbb{Q}_0$  be the initial data distribution, that is, the distribution belonging to the data’s density  $q_0$ , and let  $\mathbb{Q}_t$  be the marginal latent distribution in time  $t$  in the forward process. We also use the notation  $\mathbb{Q}_{t,t+1}$  as the joint distribution over the time  $t$  to  $t+1$  and  $\mathbb{Q} := \mathbb{Q}_{0,\dots,T}$  as the overall joint distribution over the time  $T$ . In the forward process, white Gaussian noise is gradually added to the data with  $\mathbf{x}_t = \sqrt{1 - \beta_t} \mathbf{x}_{t-1} + \sqrt{\beta_t} \mathbf{w}_t$ , where  $\mathbf{w}_t \sim \mathcal{N}(\mathbf{0}_d, \mathbb{I}_d)$  and  $\beta_t \in (0, 1)$  captures the “amount of noise” that is injected at time step  $t$  and are called the noise schedule. This can be written as the conditional distribution

$$\mathbb{Q}_{t|t-1}(\mathbf{x}_t | \mathbf{x}_{t-1}) = \mathcal{N}(\mathbf{x}_t; \sqrt{1 - \beta_t} \mathbf{x}_{t-1}, \beta_t \mathbb{I}_d).$$

An immediate result is that

$$\mathbb{Q}_t(\mathbf{x}_t | \mathbf{x}) = \mathcal{N}(\mathbf{x}_t; \sqrt{\bar{\alpha}_t} \mathbf{x}, (1 - \bar{\alpha}_t) \mathbb{I}_d),$$

for  $\alpha_t = 1 - \beta_t$  and  $\bar{\alpha}_t = \prod_{i=1}^t \alpha_i$ . For large enough  $T$  we have  $\mathbb{Q}_T \approx \mathcal{N}(\mathbf{0}_d, \mathbb{I}_d)$ . We also denote  $q_t(\mathbf{x}_t|\mathbf{x})$  as the corresponding density of  $\mathbb{Q}_t(\mathbf{x}_t|\mathbf{x})$  and that  $q_t(\mathbf{x}_t) = \int q_t(\mathbf{x}_t|\mathbf{x})q_0(\mathbf{x})d\mathbf{x}$ , in which,  $q_0$  is the unknown target density for  $\mathbf{x}$ . We also assume that  $\mathbb{Q}_0$  is absolutely continuous w.r.t. the Lebesgue measure and so the absolute continuity is preserved for all  $t \in \{1, \dots, T\}$  due to the Gaussian nature of the noise. The goal of the reverse process in diffusion models is then to generate samples (approximately) from the distribution  $\mathbb{Q}_0$  starting from the Gaussian distribution  $\mathbf{x}_T \sim \mathcal{N}(\mathbf{0}_d, \mathbb{I}_d) =: P_T$ . Let's first define

$$\mathbf{u}_t(\mathbf{x}_t) := \frac{1}{\sqrt{\alpha_t}}(\mathbf{x}_t + (1 - \alpha_t)\nabla_{\mathbf{x}_t} \log q_t(\mathbf{x}_t)).$$

At each time step, we then consider the reverse process (for sampling), specifically Langevin dynamics, which can generate samples from a probability density using the true score function, as follows:

$$\begin{aligned} \mathbf{x}_{t-1} &= \frac{1}{\sqrt{\alpha_t}}(\mathbf{x}_t + (1 - \alpha_t)\nabla_{\mathbf{x}_t} \log q_t(\mathbf{x}_t)) + \sqrt{\frac{1 - \alpha_t}{\alpha_t}}\mathbf{z}_t \\ &= \mathbf{u}_t(\mathbf{x}_t) + \sigma_t\mathbf{z}_t \end{aligned}$$

for  $\mathbf{z}_t \sim \mathcal{N}(\mathbf{0}_d, \mathbb{I}_d)$  and  $\sigma_t := \sqrt{1 - \alpha_t/\alpha_t}$ . Let's  $P_t$  be the marginal distribution of  $\mathbf{x}_t$  in the true reverse process, which is the reverse process by employing the true scores  $\nabla_{\mathbf{x}_t} \log q_t(\mathbf{x}_t)$ , and  $p_t$  be the corresponding density. Then, above statement can be written as  $P_{t-1|t} = \mathcal{N}(\mathbf{x}_{t-1}; \mathbf{u}_t(\mathbf{x}_t), \sigma_t^2\mathbb{I}_d)$ . But in practice, one does not have access to the true scores  $\nabla_{\mathbf{x}_t} \log q_t(\mathbf{x}_t)$ , instead, an estimate of it namely  $\mathbf{s}_\Theta(\cdot, t)$ , which corresponds to a neural network parameterized with a tuple  $\Theta \in \mathcal{B}$  (tuple of weight matrices), implying

$$\hat{\mathbf{u}}_t(\mathbf{x}_t) := \frac{1}{\sqrt{\alpha_t}}(\mathbf{x}_t + (1 - \alpha_t)\mathbf{s}_\Theta(\mathbf{x}_t, t)).$$

Let's  $\hat{P}_t$  be the marginal distribution of  $\mathbf{x}_t$  in the estimated reverse process implying  $\hat{P}_{t-1|t} = \mathcal{N}(\mathbf{x}_{t-1}; \hat{\mathbf{u}}_t(\mathbf{x}_t), \sigma_t^2\mathbb{I}_d)$ . For  $\mathbb{Q}_0$  absolutely continuous, we are then interested measuring the mismatch between  $\mathbb{Q}_0$  and  $\hat{P}_0$  through the Kullback–Leibler divergence

$$\text{KL}(\mathbb{Q}_0||P_0) := \mathbb{E}_{X \sim \mathbb{Q}_0} \left[ \log \frac{q_0(X)}{p_0(X)} \right] \geq 0.$$

### 3. Regularizing denoising score matching

A promising avenue for accelerating sampling in diffusion models is high-dimensional statistics (Lederer, 2022). High-dimensional statistics is a branch of statistics that deals with many variables. A key idea in high-dimensional statistics is the concept of sparsity; broadly speaking, it means that among those many variables, only few are relevant to a

problem at hand. There are different sparsity-related approaches in deep learning, such as dropout (Hinton et al., 2012; Molchanov et al., 2017; Labach et al., 2019; Gomez et al., 2019) or explicit regularization (Alvarez and Salzmann, 2016; Feng and Simon, 2017). The latter approach adds prior functions (“penalties”, “regularization”) to the objective functions of the estimators. These penalties push the estimators toward specific parts of the parameter space that correspond to certain assumptions, for example, sparsity in  $\ell_0$ -norm and/or  $\ell_1$ -norm (Lederer, 2022). The benefits of sparsity are well-documented in regression, deep learning, and beyond (Eldar and Kutyniok, 2012; Hastie et al., 2015; Neyshabur et al., 2015; Golowich et al., 2018; Schmidt-Hieber, 2020; Hebiri et al., 2025; Golestaneh et al., 2025). However, sparsity-inducing prior functions are abundant in statistics and machine learning, they are rarely employed for generative models (Lin et al., 2016). In this paper, we examine the advantages of incorporating regularization into the objective functions of score-based diffusion models. Additionally, we leverage techniques from empirical process theory (van de Geer, 2000; Vershynin, 2018) to analyze regularized objectives and calibrate the tuning parameter.

#### 3.1. $\ell_1$ -regularized denoising score matching

Here we propose an  $\ell_1$ -regularized estimator for diffusion models, inspired by the concept of “scale regularization” in deep learning (Taheri et al., 2021). Consider the parameter space

$$\mathcal{B}_1 := \left\{ \Theta \in \mathbb{R}^p : \|\mathbf{s}_\Theta(\mathbf{x}_t, t)\|_1 \leq 1 \quad \forall \mathbf{x}_t \in \mathbb{R}^d, \right. \\ \left. t \in \{1, \dots, T\} \right\}, \quad (2)$$

where  $\mathbf{s}_\Theta(\cdot, \cdot) : (\mathbb{R}^d, \mathbb{N}) \rightarrow \mathbb{R}^d$  is modeled as a neural network with two inputs, parameterized by a tuple  $\Theta = (W_0, \dots, W_L)$ . Here,  $\Theta$  collects all the weight matrices of the network, which has  $L$  hidden layers and input and output dimensions in  $\mathbb{R}^d$ . We consider  $\mathbf{s}_\Theta(\cdot, \cdot)$  as a time-dependent score-based model approximating  $\nabla_{\mathbf{x}_t} \log q_t(\mathbf{x}_t)$ , which is crucial for sample generation in the backward process of diffusion models. The parameter space  $\mathcal{B}_1$  corresponds to sparse score functions, more specifically, the outputs of these networks are sparse. Motivated by the denoising score matching objective, a scalable alternative to the objective function in (1) (Vincent, 2011), we define a regularized denoising score-matching estimator as

$$\begin{aligned} (\hat{\ell}_1, \hat{\kappa}) \in \arg \min_{\substack{\Theta \in \mathcal{B}_1 \\ \kappa \in (0, \infty)}} \mathbb{E}_{t \sim \mathcal{U}_{[0, T]}} \mathbb{E}_{X_t \sim \mathbb{Q}_t} \|\kappa \mathbf{s}_\Theta(X_t, t) - \nabla_{X_t} \log q_t(X_t)\|^2 \\ + r\kappa^2, \end{aligned} \quad (3)$$

where  $\kappa \in (0, \infty)$  represents the scale of the score function,  $r \in [0, \infty)$  is a tuning parameter that balances the penalty between scale and score matching, and  $\mathcal{U}_{[0, T]}$  de-

notes the uniform distribution over  $[0, T]$ . The fixed constraint  $\Theta \in \mathcal{B}_1$  enforces  $\ell_1$ -norm regularization, while the actual regularization concerns only on the scale  $\kappa \in (0, \infty)$ . Additionally, we regularize  $\kappa^2$  to simplify our proofs. We will further elaborate in Section A.2 on how the objective function in (3) can be computed in practice in terms of expectation and score functions.

Our main contribution in this paper is to theoretically and numerically demonstrate that our proposed regularized estimator in (3) can accelerate the sampling process of diffusion models, specifically increasing the rate of convergence in Kullback–Leibler divergence from  $d^2/\tau$  (Li et al., 2024b) or  $d^{1.5}/\tau$  (Liang et al., 2024) to  $s^2/\tau$ , where  $s \ll d$ .

We are now ready to introduce some assumptions and present our main theorem for our proposed estimator in (3).

We first set the learning rates to be used for our theory and analyses. For sufficiently large  $T$ , we set the step size  $\alpha_t$  as

$$1 - \alpha_t \approx \frac{\log T}{T}, \quad \forall t \in \{1, \dots, T\}. \quad (4)$$

We then impose some standard assumptions on the true density function.

**Assumption 3.1** (Finite Second Moment). There exists a constant  $M < \infty$  such that  $\mathbb{E}_{X_0 \sim \mathbb{Q}_0} \|X_0\|^2 \leq M$ .

Assumption 3.1 be employed in the proof of our main theorem for the convergence of the forward process ensuring that the distribution is not excessively heavy-tailed. The same assumption is also utilized in previous works including Chen et al. (2023a), Chen et al. (2023d), Benton et al. (2024), and Liang et al. (2024).

**Assumption 3.2** (Absolute Continuity). We assume that  $\mathbb{Q}_0$  is absolutely continuous w.r.t. the Lebesgue measure, and thus  $q_0$  exists.

We then push an assumption over the true gradient vectors  $\nabla_{\mathbf{x}_t} \log q_t(\mathbf{x}_t)$  for  $t \in \{1, \dots, T\}$ , that is, assuming they can be well approximated by some sparse versions. More precisely, we assume that only a small subset of features or directions in the high-dimensional space contributes significantly to the score functions. Assumption 3.3 is well-motivated in high-dimensional statistics and is central to our main Theorem 3.5.

**Assumption 3.3** (Sparsity). There is a sparsity level  $s \in \{1, 2, \dots\}$  and an accuracy  $\epsilon \in (0, \infty)$ ,  $\epsilon \leq 1/T$ , such that for all  $t \in \{1, \dots, T\}$ , there is an analytic auxiliary function  $q_t^s(\mathbf{x}_t)$  and the corresponding score  $\nabla_{\mathbf{x}_t} \log q_t^s(\mathbf{x}_t)$  that is  $s$ -sparse and  $\epsilon$ -accurate:

$$\begin{aligned} \mathbb{E}_{X_t \sim \mathbb{Q}_t} \|\nabla_{X_t} \log q_t^s(X_t)\|_0 &\leq s \text{ and} \\ \frac{1}{T} \sum_{t=1}^T \sqrt{\mathbb{E}_{X_t \sim \mathbb{Q}_t} \|\nabla_{\mathbf{x}_t} \log q_t(X_t) - \nabla_{\mathbf{x}_t} \log q_t^s(X_t)\|^2} &\leq \epsilon. \end{aligned}$$

We then assume that the derivatives of true log densities are regular, that is, they are bounded by a constant  $B \in (0, \infty)$ .

**Assumption 3.4** (Regular Derivatives). For all  $t \in \{1, \dots, T\}$  and  $l \in \{1, 2, \dots\}$  and  $\mathbf{a} \in [d]^p$  such that  $|\mathbf{a}|_1 = p \in \{1, 2, \dots\}$ , it holds that

$$\begin{aligned} \mathbb{E}_{X_t \sim \mathbb{Q}_t} |\partial_{\mathbf{a}}^p \log q_t(X_t)|^\ell &\leq B \text{ and} \\ \mathbb{E}_{X_t \sim \mathbb{Q}_t} |\partial_{\mathbf{a}}^p \log q_t(\mathbf{u}_t(X_t))|^\ell &\leq B \end{aligned}$$

for a constant  $B \in (0, \infty)$ .

The regularity Assumption 3.4 is required for our analysis in Lemma 4.1 and also is utilized in previous works like Huang et al. (2024). As discussed extensively in Liang et al. (2024, Section 5), this assumption is relatively mild, for example for distributions with finite variance or Gaussian mixtures.

**Theorem 3.5** (Non-asymptotic rates of convergence for regularized diffusion models). *Under the Assumptions 3.1, 3.2, 3.3, and 3.4 and for  $r \geq r^* := 8\sqrt{2} \log(n)/n$ , our estimator proposed in (3) generates samples with*

$$\begin{aligned} \text{KL}(\mathbb{Q}_0 \|\widehat{P}_0) &\leq \frac{cM}{T^2} + \frac{c}{T} \max\{1, (sB)^2\} \\ &+ \frac{\log T}{T} \sum_{t=1}^T \inf_{\substack{\Theta \in \mathcal{B}_1 \\ \kappa \in (0, \infty)}} \left\{ \frac{1}{n} \sum_{i=1}^n \|\kappa \mathbf{s}_{\Theta}(\mathbf{x}_t^i, t) - \nabla_{\mathbf{x}_t} \log q_t(\mathbf{x}_t^i)\|^2 \right. \\ &\left. + r\kappa^2 \right\} + sB^2 \frac{\sqrt{2 \log(nT)}}{n} + \Delta_T(\log q, \log q^s) \end{aligned}$$

for a constant  $c \in (0, \infty)$  and  $\Delta_T(\log q, \log q^s) := \sum_{t=1}^T (\mathbb{E}_{X_t \sim \mathbb{Q}_t} [\mathbb{E}_{X_{t-1} \sim \mathbb{Q}_{t-1}|t} [\log q_{t-1}(X_{t-1}) - \log q_{t-1}^s(X_{t-1})] - \mathbb{E}_{X_{t-1} \sim P_{t-1}^s} [\log q_{t-1}(X_{t-1}) - \log q_{t-1}^s(X_{t-1})]])$  with probability at least  $1 - 1/n^2$ .

**Corollary 3.6** (Parametric setting). *Assume that  $r = r^*$  and that there exists a pair  $(\Theta^*, \kappa^*) \in \mathcal{B}_1 \times (0, \infty)$  such that  $\kappa^* \mathbf{s}_{\Theta^*}(\mathbf{x}_t^i, t) = \nabla_{\mathbf{x}_t} \log q_t(\mathbf{x}_t^i)$  for all  $i \in \{1, \dots, n\}$  and  $t \in \{1, \dots, T\}$ . Then, under the Assumptions of Theorem 3.5, our estimator proposed in (3) generates samples with*

$$\begin{aligned} \text{KL}(\mathbb{Q}_0 \|\widehat{P}_0) &\leq \frac{c}{T} \max\{1, (sB)^2\} \\ &+ \frac{\log(nT)}{n} \max\{(sB)^2, (\kappa^*)^2\} + \Delta_T(\log q, \log q^s) \end{aligned}$$

for a constant  $c \in (0, \infty)$  with probability at least  $1 - 1/n^2$ .

Our Theorem 3.5 reveals that if the true gradient vectors  $\nabla_{\mathbf{x}_t} \log q_t(\mathbf{x}_t)$  can be well approximated by  $s$ -sparse vectors  $\nabla_{\mathbf{x}_t} \log q_t^s(\mathbf{x}_t)$  and for sufficiently large tuning parameter, the rates of convergence of diffusion models scale with  $s$ , where  $s \ll d$  (and not  $d$ ). The term  $\Delta_T(\log q, \log q^s)$  in the bound of Theorem 3.5 measures how close the log

density  $\log q_t(\mathbf{x}_t)$  is to the auxiliary log density  $\log q_t^s(\mathbf{x}_t)$  across the entire sample space and time steps. Note that we use the notation  $P_t^s$  for the distribution of the latent steps in the reverse process, utilizing the sparse scores of Assumption 3.3 (see also Section B.1 for more details). Following the intuition behind score matching, we argue that Assumption 3.3 also promotes closeness between these log densities. Furthermore, our empirical observations in Section 6 support the practical validity of our assumptions. Theorem 3.5 also directly implies a bound on the total-variation distance between  $\mathbb{Q}_0$  and  $\widehat{P}_0$  in view of Pinsker’s inequality. Detailed proof of Theorem 3.5 is provided in Appendix B.2. Corollary 3.6 follows directly from Theorem 3.5, so we omit its proof.

Assuming the bound  $\sum_{t=1}^T \mathbb{E}_{X_t \sim \mathbb{Q}_t} \|s(X_t, t) - \nabla_{X_t} \log q_t(X_t)\|^2 / T \leq \varsigma$ , works like Li et al. (2024b) and Liang et al. (2024) show that the reverse diffusion process produces a sample with error roughly at the order of  $\varsigma$ . But whether such accurate estimators are available in practice remains unclear. For example, Zhang et al. (2024, Theorem 3.5, Corollary 3.7) upper bounds the estimation error of the score (using  $n$  training samples) of the order of  $n^{-2\beta/(2\beta+d)}$  assuming the true data distribution  $q_0$  is 1.  $\sigma_0$ -sub-Gaussian and 2. in the Sobolev class of density functions with the order of smoothness  $\beta \leq 2$ , see also Wibisono et al. (2024); Dou et al. (2024). This result highlights that the original score matching method suffers from the curse of dimensionality (note that  $\beta \leq 2 \ll d$ ). Thus, regularization might not only accelerate the reverse process but also help in the estimation of the scores—compare to Lederer and Oesting (2023).

## 4. Technical results

Here we provide some auxiliary results used in the proof of Theorem 3.5.

**Lemma 4.1** (Reverse-step error). *Under the Assumption 3.3 and Assumption 3.4 we have for a constant  $c \in (0, \infty)$*

$$\begin{aligned} & \sum_{t=1}^T \mathbb{E}_{X_t, X_{t-1} \sim \mathbb{Q}_{t,t-1}} \left[ \log \frac{q_{t-1|t}(X_{t-1}|X_t)}{p_{t-1|t}^s(X_{t-1}|X_t)} \right] \\ & \leq \frac{c}{T} (sB^2 + s^2B^2 + s^2B^2\epsilon) + c\sqrt{s}B\epsilon \\ & \quad + \Delta_T(\log q, \log q^s). \end{aligned}$$

Lemma 4.1 helps upper bounding the reverse-step error for the backward process of diffusion models and its detailed proof is provided in Appendix B.3.

We then present a lemma that aids in determining the optimal rates for the tuning parameter.

**Lemma 4.2** (Empirical processes). *Under the Assump-*

*tion 3.3 we obtain*

$$\begin{aligned} & \sup_{\Theta \in \mathcal{B}_1} \left| \mathbb{E}_{X_t \sim \mathbb{Q}_t} \|\hat{\kappa} s_{\Theta}(X_t, t) - \nabla \log q_t^s(X_t)\|^2 \right. \\ & \quad \left. - \frac{1}{n} \sum_{i=1}^n \|\hat{\kappa} s_{\Theta}(\mathbf{x}_t^i, t) - \nabla \log q_t^s(\mathbf{x}_t^i)\|^2 \right| \\ & \leq 8(\hat{\kappa}^2 + sB^2) \sqrt{\frac{2 \log n}{n}} \end{aligned}$$

*with probability at least  $1 - 32/n^2$ .*

Lemma 4.2 is employed in the proof of Theorem 3.5 to calibrate the tuning parameter. Its detailed proof is provided in Appendix B.4.

## 5. Related work

The non-asymptotic rates of convergence for diffusion models established very recently (Block et al., 2020; De Bortoli et al., 2021; De Bortoli, 2022; Lee et al., 2022; Chen et al., 2023c;a; Li et al., 2024b; Chen et al., 2023e; Huang et al., 2024) show the large interest in this topic and are an important step forward but do not fully explain the success of generative models either. For example, results like Block et al. (2020, Theorem 13) provide rates of convergence for diffusion models in terms of Wasserstein distance employing the tools from empirical-process theory, but they suffer from the curse of dimensionality in that the rates depend exponentially on the dimensions of the data, that is, the number of input features. Recent works then concentrate on improving convergence guarantees to grow polynomially in the number of input features under different assumptions on the original and estimated scores ( $L_2$ -accurate score estimates, Lipschitz or smooth scores, scores with bounded moments) (Lee et al., 2022; Wibisono and Yang, 2022; Chen et al., 2023d;c;a;e; Lee et al., 2023; Huang et al., 2024). For example, Lee et al. (2022) prove a convergence guarantee in terms of total variation for SGMs, which has a polynomial dependence on the number of input features if the score estimate is  $L_2$ -accurate for any smooth distribution satisfying the log-Sobolev inequality. A very recent work by Li et al. (2024b) proposes improved convergence rates in terms of total variation for DDPMs with ordinary differential equations and stochastic differential equations samplers that are proportional to  $d^2/\tau$ , where  $d$  is the number of input features and  $\tau$  the error in the measure under consideration. They assumed 1. finite support assumption, 2.  $L_2$ -accurate score estimates, and 3. accurate Jacobian matrices. Li et al. (2024b, Theorem 3) also provides rates growing by  $d^3/\sqrt{\tau}$  for an accelerated ordinary differential equations samplers.

While works like Li et al. (2024b) and Li et al. (2024a) concentrate more on improving the rates in  $\tau$ , Chen et al. (2023c) focus on improving the rates in  $d$  for denoising diffusion implicit models. Chen et al. (2023c) use a specially

chosen corrector step based on the underdamped Langevin diffusion to achieve their improvements, namely rates proportional to  $L^2\sqrt{d}/\tau$  by assuming: 1. the score function along the forward process is  $L$ -Lipschitz, 2. finite second moments of the data distribution, and 3.  $L_2$ -accurate score estimates. [Chen et al. \(2023a\)](#); [Benton et al. \(2024\)](#) then relaxed the assumptions over the data distribution and proposed the rates of convergence for DDPM proportional to  $\sqrt{d^2/\tau}$  and  $\sqrt{d}/\tau$  under 1. finite second moments of the data distribution, and 2.  $L_2$ -accurate score estimates. Further research directions may also build upon [Chen et al. \(2023b\)](#), who assume that the data lie on a low-dimensional linear subspace. They demonstrate that, in this setting, the convergence rates depend on the dimension of the subspace.

## 6. Empirical support

In this section, we demonstrate the benefits of regularization for diffusion empirically. Rather than relying on large-scale pipelines and data, which are subject to a number of other factors, we study the influence of regularization in simple, well-explored setups. We present a toy example and the MNIST family dataset here, deferring additional simulations and setups to Appendix Section A.

### 6.1. Toy example

We first highlight the influence of regularization on the sampling process of a 3D toy example. We consider 2000 three-dimensional, independent Gaussian samples with mean zero and covariance matrix  $[0.08, 0, 0; 0, 1, 0; 0, 0, 1]$ ; hence, the data fluctuate most around the  $y$  and  $z$  axes. We then train two diffusion models, with the same data: the original denoising score matching and the same with an additional sparsity-inducing regularization (as proposed in (3)) and  $r = 0.001$ . Figure 1 visualizes the data (first panel) and the sampling process with  $T = 60$  for original score matching (second panel) and the regularized version (third panel). Both models start from the blue dot. The figure shows that the regularized version provides a more focused sampling.

### 6.2. MNIST

We now compare original score matching and the regularized version on MNIST dataset ([LeCun et al., 1998](#)) including  $n = 50\,000$  training samples. We are interested to time steps  $T \in \{500, 50, 20\}$  for sampling and we consider regularization with  $r = 0.0005$  for  $T = 500$  and  $r = 0.003$  for  $T \in \{50, 20\}$ . In fact, we set the tuning parameter as a decreasing function of  $T$ , let say  $r = f[T] \in O(c'/T)$  for a real constant  $c \in (0, \infty)$ . Note that two models are already trained over the same amount of data and identical settings employing different objectives. For sampling (starting from pure noise), then we try different values of time steps  $T \in \{500, 50, 20\}$ . That means, for small values of

$T$ , we just need to pick up a **larger step size** as we always start from pure noise (see Algorithm 2). Figure 2 shows the results. While the original score matching fails to generate reasonable samples for small values of  $T$ , our proposed score function performs successfully even for  $T = 20$ . In all our simulations, we use the same network structure, optimization method, and sampling approach with identical settings for both approaches (see Appendix A.3 for detailed settings). The only difference lies in the objective functions: one is regularized, while the other is not. While it could be argued that alternative network structures or sampling processes might enhance the quality of the generated images for original score matching, our focus remains on the core idea of regularization fixing all other factors and structures. We defer the enhanced versions of our simulations aimed at achieving higher-quality images to future works.

### 6.3. FashionMNIST

We follow almost all the settings as in Section 6.2 with  $r = 0.0001$  for  $T = 500$  and  $r = 0.002$  for  $T \in \{70, 50\}$  for FashionMNIST dataset ([Xiao et al., 2017](#)) including  $n = 50\,000$  training samples. Results are provided in Figures 3. Following the generated images obtained using both approaches, and ensuring that all factors except the objective functions remain identical, we observe that the original score-matching approach produces samples that appear oversmoothed and exhibit imbalanced distributions (see the first image of the left panel of Figure 3). In contrast, our regularized approach with a considerably small tuning parameter, generates images that resemble the true data more closely and exhibit a more balanced distribution (see the first image of the right panel of Figure 3). For instance, the percentages of generated images for Sandals, Trousers, Dresses, Ankle Boots, and Bags are approximately  $(0.0, 0.7, 2.0, 3.0, 4.0)$  using the original score matching, compared to  $(8.0, 6.0, 8.0, 10.0, 10.0)$  with the regularized version, highlighting the clear imbalance in distribution for the original score matching.

## 7. Conclusion

Our mathematical proofs (Section 3) and empirical illustrations (Section 6) demonstrate that regularization can reduce the computational complexity of diffusion models considerably. Broadly speaking, regularization replaces the dependence on the input dimension by a dependence on a much smaller intrinsic dimension. But our findings might just be the beginning: we believe that types of regularization beyond the sparsity-inducing  $\ell_1$ -regularization applied here, such as total variation, could lead to further improvements.

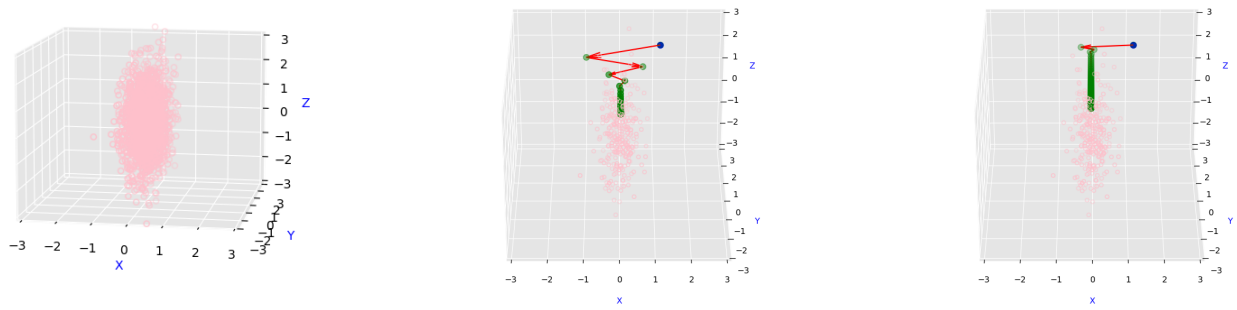


Figure 1. Visualizing the sampling process for 3D data (first panel) with original denoising score matching (second panel) versus regularized denoising score matching (third panel). The original samples are depicted as red circles, blue circles indicate the starting points for sampling, and green circles represent the latent generated samples. The red arrows illustrate the sampling paths. It is evident that regularized denoising score matching predominantly adheres to the two-dimensional sub-manifold (along the  $Y$  and  $Z$  axes), whereas the original denoising score matching explores the entire 3D space.

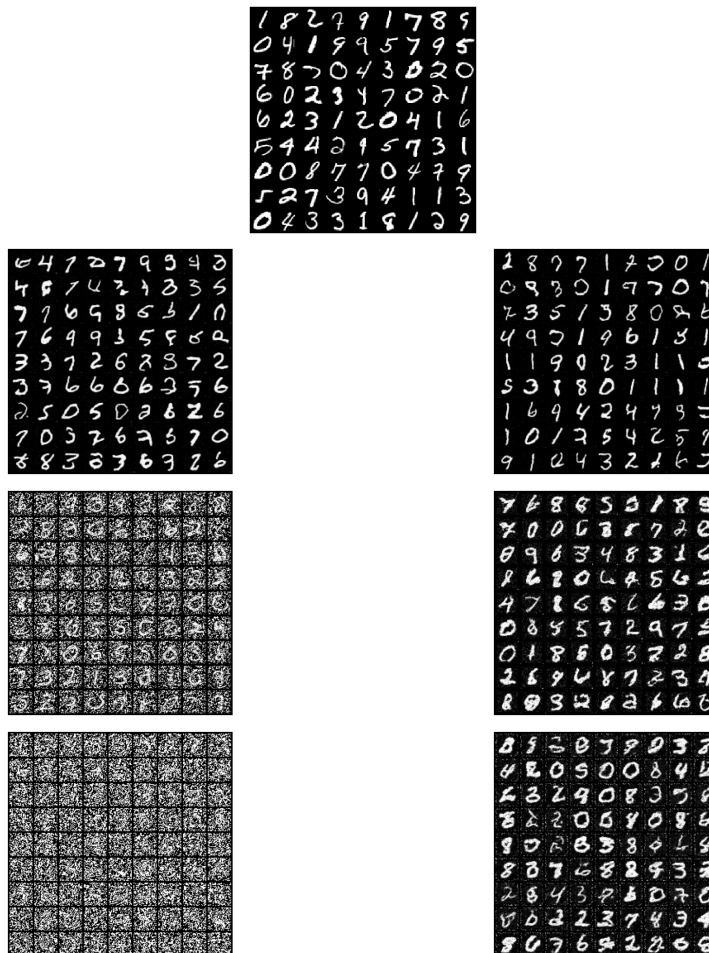


Figure 2. Image generation using the original denoising score matching (left column) versus the regularized version (right column) for different time steps,  $T = 500$ ,  $T = 50$ , and  $T = 20$  (from top to bottom). The middle column displays 81 original samples from the MNIST dataset for comparison with images of dimensions  $d = 28 \times 28 \times 1 = 784$ . Our regularized version generates high-quality images for  $T = 500$  (comparable to the original denoising score matching) and still produces good images for small  $T$ , while the original denoising score matching totally fails.

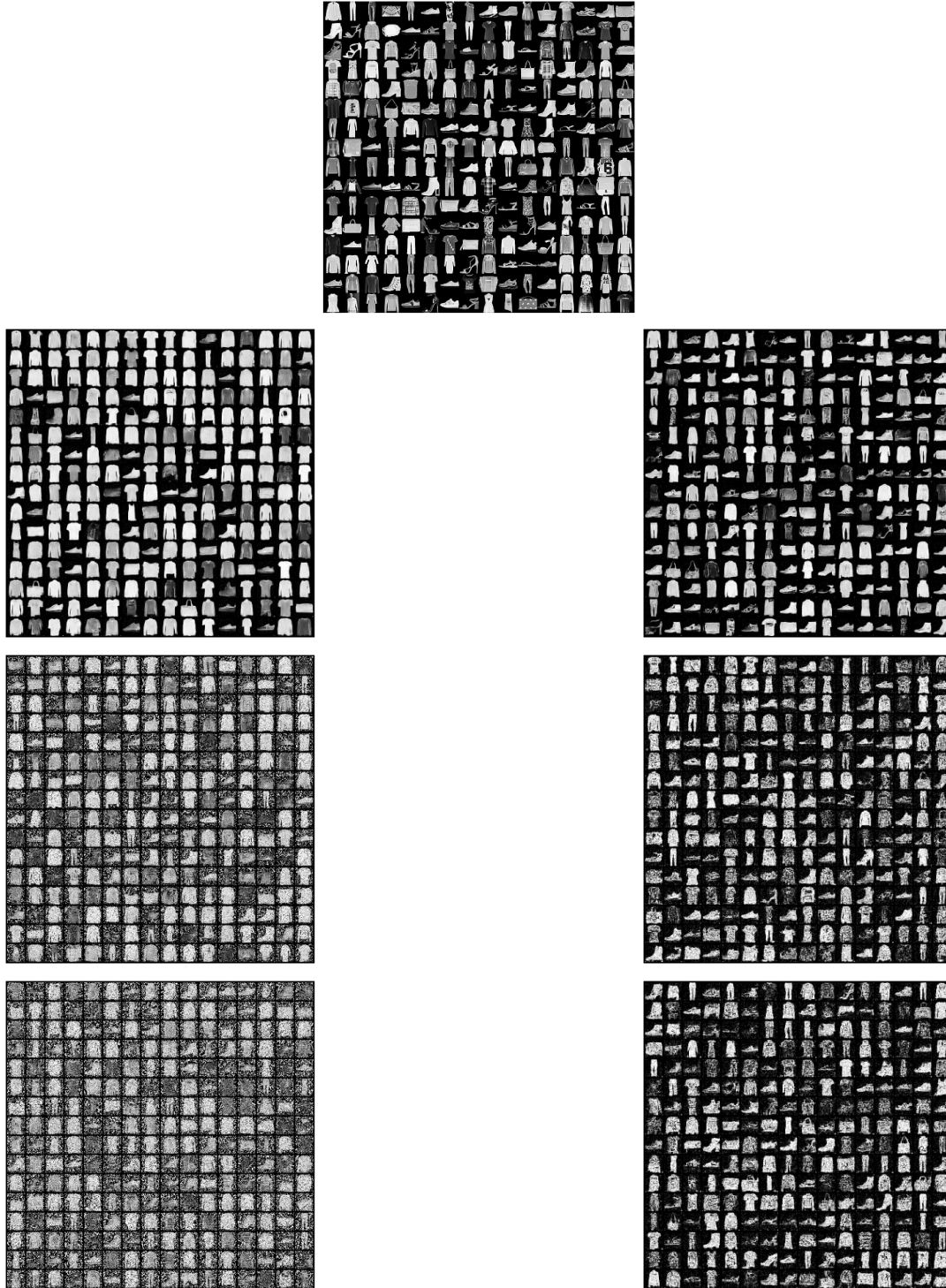


Figure 3. Image generation using the original denoising score matching (left column) versus the regularized version (right column) for different time steps,  $T = 500$ ,  $T = 70$ , and  $T = 50$  (from top to bottom). The middle column displays 256 original samples from the FashionMNIST dataset for comparison with images of dimensions  $d = 28 \times 28 \times 1 = 784$ . Our regularized version generates high-quality images for  $T = 500$  (comparable to the original denoising score matching) and still produces good images even for small  $T$ , while the original denoising score matching totally fails. Another notable observation is that our regularization results in more balanced image generation, as evident when comparing our method to the original denoising score matching at  $T = 500$ , where the latter produces overly smooth images.



---

## Acknowledgements

This research was partially funded by grants 502906238, 543964668 (SPP2298), and 520388526 (TRR391) by the Deutsche Forschungsgemeinschaft (DFG, German Research Foundation).

## References

- J. Alvarez and M. Salzmann. Learning the number of neurons in deep networks. In *Proc. NIPS*, pages 2270–2278, 2016.
- J. Benton, V. De Bortoli, A. Doucet, and G. Deligiannidis. Linear convergence bounds for diffusion models via stochastic localization. *Proc. ICLR*, 2024.
- A. Block, Y. Mroueh, and A. Rakhlin. Generative modeling with denoising auto-encoders and langevin sampling. *arXiv:2002.00107*, 2020.
- H. Chen, H. Lee, and J. Lu. Improved analysis of score-based generative modeling: User-friendly bounds under minimal smoothness assumptions. In *Proc. ICML*, pages 4735–4763, 2023a.
- M. Chen, K. Huang, T. Zhao, and M. Wang. Score approximation, estimation and distribution recovery of diffusion models on low-dimensional data. In *Proc. ICML*, pages 4672–4712. PMLR, 2023b.
- S. Chen, S. Chewi, H. Lee, Y. Li, J. Lu, and A. Salim. The probability flow ode is provably fast. In *Proc. NIPS*, volume 36, 2023c.
- S. Chen, S. Chewi, J. Li, Y. Li, A. Salim, and A. Zhang. Sampling is as easy as learning the score: theory for diffusion models with minimal data assumptions. In *Proc. ICLR*, 2023d.
- S. Chen, G. Daras, and A. Dimakis. Restoration-degradation beyond linear diffusions: A non-asymptotic analysis for ddim-type samplers. In *Proc. ICML*, pages 4462–4484. PMLR, 2023e.
- V. De Bortoli. Convergence of denoising diffusion models under the manifold hypothesis. *arXiv:2208.05314*, 2022.
- V. De Bortoli, J. Thornton, J. Heng, and A. Doucet. Diffusion schrödinger bridge with applications to score-based generative modeling. In *Proc. NIPS*, volume 34, pages 17695–17709, 2021.
- P. Dhariwal and A. Nichol. Diffusion models beat gans on image synthesis. In *Proc. NIPS*, volume 34, pages 8780–8794, 2021.
- Z. Dou, S. Kotekal, Z. Xu, and H. Zhou. From optimal score matching to optimal sampling. *arXiv:2409.07032*, 2024.
- Y. Eldar and G. Kutyniok, editors. *Compressed Sensing: Theory and Applications*. Cambridge Univ. Press, 2012.
- J. Feng and N. Simon. Sparse-input neural networks for high-dimensional nonparametric regression and classification. *arXiv:1711.07592*, 2017.
- P. Golestaneh, M. Taheri, and J. Lederer. How many samples are needed to train a deep neural network? *Proc. ICLR*, 2025.
- N. Golowich, A. Rakhlin, and O. Shamir. Size-independent sample complexity of neural networks. In *Proc. COLT*, pages 297–299, 2018.
- A. Gomez, I. Zhang, S. Kamalakar, D. Madaan, K. Swersky, Y. Gal, and G. Hinton. Learning sparse networks using targeted dropout. *arXiv:1905.13678*, 2019.
- T. Hastie, R. Tibshirani, and M. Wainwright. *Statistical learning with sparsity: The lasso and generalizations*. CRC press, 2015.
- M. Hebiri, J. Lederer, and M. Taheri. Layer sparsity in neural networks. *J. Statist. Plann. Inference*, 234:106195, 2025. ISSN 0378-3758.
- G. Hinton, L. Deng, D. Yu, G. Dahl, A. Mohamed, N. Jaitly, A. Senior, V. Vanhoucke, P. Nguyen, T. Sainath, and B. Kingsbury. Deep neural networks for acoustic modeling in speech recognition: The shared views of four research groups. *IEEE Signal Process. Mag.*, 29(6):82–97, 2012.
- J. Ho, A. Jain, and P. Abbeel. Denoising diffusion probabilistic models. In *Proc. NIPS*, volume 33, pages 6840–6851, 2020.
- J. Ho, T. Salimans, A. Gritsenko, W. Chan, M. Norouzi, and D. Fleet. Video diffusion models. In *Proc. NIPS*, volume 35, pages 8633–8646, 2022.
- D. Huang, J. Huang, and Z. Lin. Convergence analysis of probability flow ode for score-based generative models. *arXiv:2404.09730*, 2024.
- A. Hyvärinen. Some extensions of score matching. *Comput. Statist. Data Anal.*, 51(5):2499–2512, 2007.
- A. Hyvärinen and P. Dayan. Estimation of non-normalized statistical models by score matching. *J. Mach. Learn. Res.*, 6(4), 2005.
- A. Labach, H. Salehinejad, and S. Valaee. Survey of dropout methods for deep neural networks. *arXiv:1904.13310*, 2019.
- Y. LeCun, L. Bottou, Y. Bengio, and P. Haffner. Gradient-based learning applied to document recognition. In *Proc. IEEE*, pages 2278–2324, 1998.

- 
- J. Lederer. *Fundamentals of High-Dimensional Statistics: with exercises and R labs*. Springer Texts in Statistics, 2022.
- J. Lederer and M. Oesting. Extremes in high dimensions: Methods and scalable algorithms. *arXiv:2303.04258*, 2023.
- M. Ledoux and M. Talagrand. *Probability in Banach Spaces: isoperimetry and processes*. Springer Science & Business Media, 2013.
- H. Lee, J. Lu, and Y. Tan. Convergence for score-based generative modeling with polynomial complexity. In *Proc. NIPS*, volume 35, pages 22870–22882, 2022.
- H. Lee, J. Lu, and Y. Tan. Convergence of score-based generative modeling for general data distributions. *ALT*, pages 946–985, 2023.
- G. Li, Y. Huang, T. Efimov, Y. Wei, Y. Chi, and Y. Chen. Accelerating convergence of score-based diffusion models, provably. *arXiv:2403.03852*, 2024a.
- G. Li, Y. Wei, Y. Chen, and Y. Chi. Towards faster non-asymptotic convergence for diffusion-based generative models. In *Proc. ICLR*, 2024b.
- Y. Liang, P. Ju, Y. Liang, and N. Shroff. Broadening target distributions for accelerated diffusion models via a novel analysis approach. *arXiv:2402.13901*, 2024.
- L. Lin, M. Drton, and A. Shojaie. Estimation of high-dimensional graphical models using regularized score matching. *Electron. J. Stat.*, 10(1):806, 2016.
- D. Molchanov, A. Ashukha, and D. Vetrov. Variational dropout sparsifies deep neural networks. In *Proc. ICML*, pages 2498–2507, 2017.
- B. Neyshabur, R. Tomioka, and N. Srebro. Norm-based capacity control in neural networks. In *Proc. COLT*, pages 1376–1401, 2015.
- A. Ramesh, P. Dhariwal, A. Nichol, C. Chu, and M. Chen. Hierarchical text-conditional image generation with clip latents. *arXiv:2204.06125*, 1(2):3, 2022.
- J. Schmidt-Hieber. Nonparametric regression using deep neural networks with relu activation function. *Ann. Statist.*, 48(4):1875–1897, 2020.
- Y. Song and S. Ermon. Generative modeling by estimating gradients of the data distribution. In *Proc. NIPS*, volume 32, 2019.
- Y. Song, S. Garg, J. Shi, and S. Ermon. Sliced score matching: A scalable approach to density and score estimation. In *Uncertainty artif. intell.*, pages 574–584. PMLR, 2020.
- Y. Song, C. Durkan, I. Murray, and S. Ermon. Maximum likelihood training of score-based diffusion models. In *Proc. NIPS*, volume 34, pages 1415–1428, 2021a.
- Y. Song, J. Sohl-Dickstein, D. Kingma, A. Kumar, S. Ermon, and B. Poole. Score-based generative modeling through stochastic differential equations. In *Proc. ICLR*, 2021b.
- M. Taheri, F. Xie, and J. Lederer. Statistical guarantees for regularized neural networks. *Neural Networks*, 142: 148–161, 2021.
- S. van de Geer. *Empirical processes in M-estimation*. Cambridge Univ. Press, 2000.
- S. van de Geer. *Estimation and testing under sparsity*. Springer, 2016.
- R. Vershynin. *High-dimensional probability: an introduction with applications in data science*. Cambridge Univ. Press, 2018.
- P. Vincent. A connection between score matching and denoising autoencoders. *Neural Comput.*, 23(7):1661–1674, 2011.
- A. Wibisono and K. Yang. Convergence in kl divergence of the inexact langevin algorithm with application to score-based generative models. *arXiv:2211.01512*, 2022.
- A. Wibisono, Y. Wu, and K. Yang. Optimal score estimation via empirical bayes smoothing. *arXiv:2402.07747*, 2024.
- H. Xiao, K. Rasul, and R. Vollgraf. Fashion-MNIST: a novel image dataset for benchmarking machine learning algorithms. *arXiv:1708.07747*, 2017.
- M. Xu, L. Yu, Y. Song, C. Shi, S. Ermon, and J. Tang. Geodiff: A geometric diffusion model for molecular conformation generation. *arXiv:2203.02923*, 2022.
- K. Zhang, C. Yin, F. Liang, and J. Liu. Minimax optimality of score-based diffusion models: Beyond the density lower bound assumptions. *arXiv:2402.15602*, 2024.

---

## A. Complementary simulations

In this section, we provide additional simulation supporting our theories on further image dataset Butterflies (Section A.1). We also introduce our training and sampling approach in Section A.2 and provide details about network architecture and training settings in Section A.3.

### A.1. Butterflies

We also compare original diffusion and regularized analog on `Butterflies` dataset (`smithsonian-butterflies`) including  $n = 10\,000$  training samples. We consider regularization  $r = 0.0001$  for  $T = 1000$  and  $r = 0.0005$  for  $T \in \{200, 150\}$ . Results are provided in Figure 4. Again, our results show that our approach perform better than the original score matching for small values of  $T$ .

### A.2. Training and sampling algorithms

Here we provide details about how we solve the objective function (3) in practice, that is, how we deal with the expected values and score functions.

Let’s first define the objective function over a batch of training examples  $\mathbf{x}_{b_s}$  (a batch of size  $b_s \in \{1, 2, \dots\}$ ) and for a batch of random time steps  $\mathbf{t}_{b_s} \in (0, 1]^{b_s}$ :

$$f(\kappa, \Theta, \mathbf{x}_{b_s}, \mathbf{t}_{b_s}) := \frac{1}{b_s} \sum_{i=1}^{b_s} \left[ \|\kappa \mathbf{s}_\Theta(\mathbf{x}_{t_i}^i, t_i) - \nabla_{\mathbf{x}_t} \log q_t(\mathbf{x}_{t_i}^i | \mathbf{x}^i)\|^2 \right] + r\kappa^2 \quad (5)$$

with

$$\mathbb{Q}_t(\mathbf{x}_{t_i}^i | \mathbf{x}^i) = \mathcal{N}(\mathbf{x}^i, \sigma_t \mathbb{I}_d) \quad (6)$$

with  $\sigma_t := (\sigma^{2t} - 1)/(2 \log \sigma)$  for  $t \in (0, 1]$  and a large enough  $\sigma \in (0, \infty)$  (we set  $\sigma = 5$  for `Butterflies` and  $\sigma = 25$  for other datasets). Here  $\mathbf{x}_t^i$  corresponds to a perturbed version of the training sample  $\mathbf{x}^i$  ( $i$ th sample of the batch) in time step  $t$ . As stated in (6), once  $\sigma$  is large,  $\mathbf{x}_1$  ( $t = 1$ ) goes to a mean-zero Gaussian. And as shown in Vincent (2011), the optimization objective  $\mathbb{E}_{q_t(\mathbf{x}_t | \mathbf{x}) q_0(\mathbf{x})} [\|\kappa \mathbf{s}_\Theta(\mathbf{x}_t, t) - \nabla_{\mathbf{x}_t} \log q_t(\mathbf{x}_t | \mathbf{x})\|^2]$  for a fixed variance  $\sigma_t$  is equivalent to the optimization objective  $\mathbb{E}_{q_t(\mathbf{x}_t)} [\|\kappa \mathbf{s}_\Theta(\mathbf{x}_t, t) - \nabla_{\mathbf{x}_t} \log q_t(\mathbf{x}_t)\|^2]$  and, therefore, satisfies  $\kappa^* \mathbf{s}_{\Theta^*}(\mathbf{x}_t, t) = \nabla_{\mathbf{x}_t} \log q_t(\mathbf{x}_t)$ . We then provide Algorithm 1 for solving the objective function in (3). Note that we can easily compute the score functions in (5) since there is a closed form solution for them as densities are just Gaussian conditional on  $\mathbf{x}^i$ .

---

#### Algorithm 1 Training algorithm

---

- 1: **Inputs:**  $\sigma, n_{\text{epochs}}$  (number of epochs),  $b_s$ (batch-size),  $\text{eps} = 0.00001$
  - 2: **Outputs:**  $(\hat{\Theta}_{\ell_1}, \hat{\kappa})$
  - 3: Initialize parameters  $(\hat{\Theta}_{\ell_1}, \hat{\kappa})$
  - 4: **for**  $i = 1$  to  $n_{\text{epochs}}$  **do**
  - 5:   **for**  $\mathbf{x}_{b_s}$  in data-loader **do**
  - 6:      $\mathbf{t}_{b_s} = \{\mathcal{U}_{[0,1]}\}^{b_s} (1 - \text{eps}) + \text{eps}$
  - 7:     One step optimization minimizing  $f(\kappa, \Theta, \mathbf{x}_{b_s}, \mathbf{t}_{b_s})$  in (5) employing a random batch of time steps  $\mathbf{t}_{b_s} \in (0, 1]^{b_s}$  and updating  $(\hat{\Theta}_{\ell_1}, \hat{\kappa})$
  - 8:   **end for**
  - 9: **end for**
- 

Parameter `eps` in Algorithm 1 is introduced for numerical stability and to refuse  $t = 0$ . For a sufficiently large number of epochs, we expect to learn the scores accurately for different time steps. For sampling process, we employ a naive sampler as proposed in Algorithm 2 employing Langevin dynamics (Song and Ermon, 2019, Section 2.2) to align with our theory.

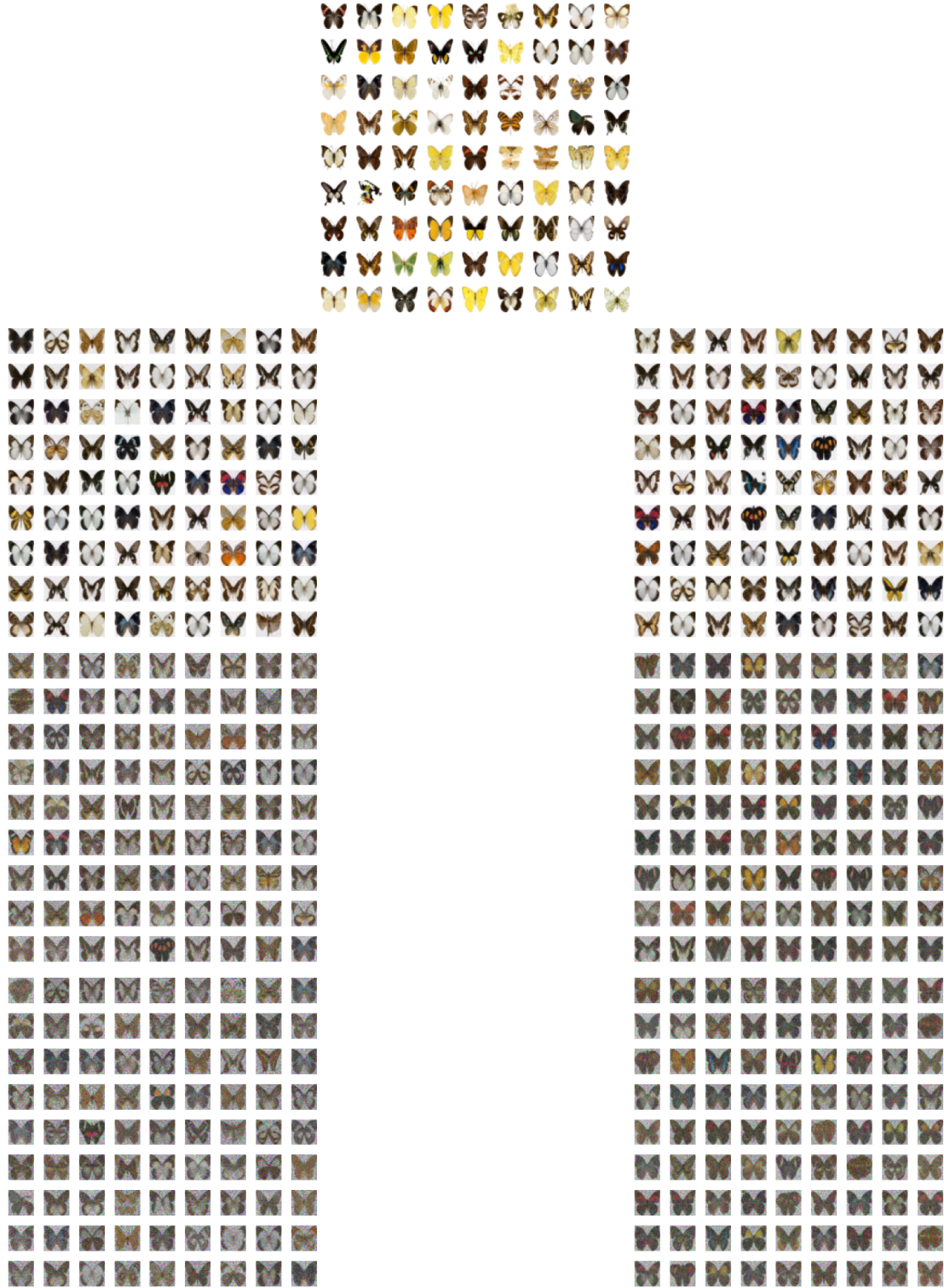


Figure 4. Image generation using the original denoising score matching (left column) versus the regularized version (right column) for different time steps,  $T = 1000$ ,  $T = 200$ , and  $T = 150$  (from top to bottom). The middle column displays 81 original samples from the Butterflies dataset for comparison. The dataset consists of images with dimensions  $d = 28 \times 28 \times 3 = 2352$ . As shown in the images, our regularized version generates high-quality images for  $T = 1000$  (comparable to the original denoising score matching) and still perform better than original denoising score matching for  $T = 200$  and  $T = 150$ .

---

**Algorithm 2** Sampling algorithm

---

- 1: **Inputs:**  $\sigma$ ,  $\text{eps} = 0.00001$ ,  $T$  (Time steps)
  - 2: **Output:**  $\mathbf{x}$
  - 3:  $\mathbf{x} = \mathbf{x}_{\text{init}} = \mathcal{N}(\mathbf{0}_d, \mathbb{I}_d)\sigma_1$
  - 4:  $\mathbf{t} = \text{linspace}(1., \text{eps}, T)$  (make a grid of time steps)
  - 5:  $\eta = \mathbf{t}[0] - \mathbf{t}[1]$  (set step size)
  - 6: **for**  $\mathbf{t}$  in  $\mathbf{t}$  **do**
  - 7:    $\mathbf{x} = \mathbf{x} + \eta \hat{\kappa} \mathbf{s}_{\hat{\Theta}_{\epsilon_1}}(\mathbf{x}, t) + \sqrt{2\eta} \mathcal{N}(\mathbf{0}_d, \mathbb{I}_d)$  (update  $\mathbf{x}$ )
  - 8: **end for**
- 

### A.3. Network architecture and training settings

Our model is a U-Net architecture with 4 downsampling and 4 upsampling layers, each comprising residual blocks. The network starts with a base width of 32 channels, doubling at each downsampling step to a maximum of 256 channels, and mirrors this in the decoder. A bottleneck layer with 256 channels connects the encoder and decoder. Time information is encoded using Gaussian Fourier projections and injected into each residual block via dense layers. Group normalization is applied within the residual blocks, and channel attention mechanisms are included selectively to enhance feature representations. For training, we used the Adam optimizer with a learning rate of 0.001, and for sampling, we employed a signal-to-noise ratio of 0.1. We used a batch size of 128 and trained for 2000 epochs on the `Butterflies` dataset and less than 1000 epochs on the other datasets.

## B. Auxiliary results and proofs

In this section, we first provide two auxiliary results and then, we present detailed proofs of our main results. Note that throughout our proofs, we will omit the index  $\mathbf{x}_t$  from  $\nabla_{\mathbf{x}_t} \log q_t(\cdot)$  for simplicity in notations and simply write  $\nabla \log q_t(\cdot)$ .

### B.1. Auxiliary results

We denote the distribution of the latent steps in the reverse process, utilizing the sparse gradient vector, as  $P_{t-1|t}^s := \mathcal{N}(\mathbf{x}_{t-1}; \mathbf{u}_t^s(\mathbf{x}_t), \sigma_t^2 \mathbb{I}_d)$  with

$$\mathbf{u}_t^s(\mathbf{x}_t) := \frac{1}{\sqrt{\alpha_t}} (\mathbf{x}_t + (1 - \alpha_t) \nabla_{\mathbf{x}_t} \log q_t^s(\mathbf{x}_t)). \quad (7)$$

We then connect the conditional distributions  $q_{t-1|t}(\mathbf{x}_{t-1}|\mathbf{x}_t)$  and  $p_{t-1|t}^s(\mathbf{x}_{t-1}|\mathbf{x}_t)$  using the following lemma inspired by proof approach of [Liang et al. \(2024\)](#):

**Lemma B.1** (Tilting factor). *For a fixed  $\mathbf{x}_t$  we have*

$$q_{t-1|t}(\mathbf{x}_{t-1}|\mathbf{x}_t) \propto p_{t-1|t}^s(\mathbf{x}_{t-1}|\mathbf{x}_t) \exp(\zeta_{t,t-1}(\mathbf{x}_t, \mathbf{x}_{t-1}))$$

with  $\zeta_{t,t-1}(\mathbf{x}_t, \mathbf{x}_{t-1}) := \log q_{t-1}(\mathbf{x}_{t-1}) - \sqrt{\alpha_t} \mathbf{x}_{t-1}^T \nabla \log q_t^s(\mathbf{x}_t) + f(\mathbf{x}_t)$ , where  $f(\mathbf{x}_t)$  is an arbitrary function of  $\mathbf{x}_t$ .

The notation  $\propto$  in the [Lemma B.1](#) means proportional. [Lemma B.1](#) is employed in the proof of our [Lemma 4.1](#) and its detailed proof is presented in [Section B.5](#).

**Lemma B.2** (Log-density of backward process). *We have*

$$\begin{aligned} & \sum_{t=1}^T \mathbb{E}_{X_t, X_{t-1} \sim Q_{t,t-1}} \left[ \log \frac{p_{t-1|t}^s(X_{t-1}|X_t)}{\hat{p}_{t-1|t}(X_{t-1}|X_t)} \right] \\ & \leq (1 - \alpha_t) \sum_{t=1}^T \left( \sqrt{\mathbb{E}_{X_t \sim Q_t} \|\nabla \log q_t(X_t) - \nabla \log q_t^s(X_t)\|^2 \mathbb{E}_{X_t \sim Q_t} \|\nabla \log q_t^s(X_t) - \hat{\kappa} \mathbf{s}_{\hat{\Theta}_{\epsilon_1}}(X_t, t)\|^2} \right. \\ & \quad \left. + \frac{1}{2} \mathbb{E}_{X_t \sim Q_t} \|\hat{\kappa} \mathbf{s}_{\hat{\Theta}_{\epsilon_1}}(X_t, t) - \nabla \log q_t^s(X_t)\|^2 \right). \end{aligned}$$

[Lemma B.2](#) is employed in the proof our main [Theorem 3.5](#) and its detailed proof is presented in [Section B.6](#).

## B.2. Proof of Theorem 3.5

*Proof.* The poof approach is based on decomposing the total error using the Markov property of the forward and the backward process. We then, employ our Lemma 4.1 and Lemma 4.2 to handle individual terms.

Following the proof approach proposed by Liang et al. (2024, Equation 13) (based on Markov property of the forward and the backward process), we can decompose the total error as

$$\text{KL}(\mathbb{Q}_0||\hat{P}_0) \leq \text{KL}(\mathbb{Q}_T||\hat{P}_T) + \sum_{t=1}^T \mathbb{E}_{X_t \sim \mathbb{Q}_t} [\text{KL}(\mathbb{Q}_{t-1|t}(\cdot|X_t)||\hat{P}_{t-1|t}(\cdot|X_t))].$$

We then employ the auxiliary function  $q_t^s(\cdot)$  that satisfies our Assumption 3.3 (it doesn't need to be necessarily unique). We also use the notation  $p_t^s(\cdot)$  for the reverse counterpart of the auxiliary function  $q_t^s(\cdot)$  (see (7)). We then rewrite the previous display employing  $p_t^s(\cdot)$  and the definition of KL:

$$\begin{aligned} \text{KL}(\mathbb{Q}_0||\hat{P}_0) &\leq \text{KL}(\mathbb{Q}_T||\hat{P}_T) + \sum_{t=1}^T \mathbb{E}_{X_t \sim \mathbb{Q}_t} [\text{KL}(\mathbb{Q}_{t-1|t}(\cdot|X_t)||\hat{P}_{t-1|t}(\cdot|X_t))] \\ &= \underbrace{\text{KL}(\mathbb{Q}_T||\hat{P}_T)}_{\text{Term 1: Initialization error}} + \underbrace{\sum_{t=1}^T \mathbb{E}_{X_t, X_{t-1} \sim \mathbb{Q}_{t,t-1}} \left[ \log \frac{q_{t-1|t}(X_{t-1}|X_t)}{p_{t-1|t}^s(X_{t-1}|X_t)} \right]}_{\text{Term 2: Reverse-step error}} \\ &\quad + \underbrace{\sum_{t=1}^T \mathbb{E}_{X_t, X_{t-1} \sim \mathbb{Q}_{t,t-1}} \left[ \log \frac{p_{t-1|t}^s(X_{t-1}|X_t)}{\hat{p}_{t-1|t}(X_{t-1}|X_t)} \right]}_{\text{Term 3: Estimation error}}. \end{aligned}$$

We now need to study each term specified above individually.

*Term 1: Initialization error*

Under the Assumption 3.1 and the assumed step size in (4), we have with Liang et al. (2024, Remark 1)

$$\text{KL}(\mathbb{Q}_T||\hat{P}_T) \leq c \frac{M}{T^2}.$$

*Term 2: Reverse-step error*

Under our Assumption 3.3 and Assumption 3.4 and with Lemma 4.1 we have

$$\begin{aligned} &\sum_{t=1}^T \mathbb{E}_{X_t, X_{t-1} \sim \mathbb{Q}_{t,t-1}} \left[ \log \frac{q_{t-1|t}(X_{t-1}|X_t)}{p_{t-1|t}^s(X_{t-1}|X_t)} \right] \\ &\leq \frac{c}{T} (sB^2 + s^2B^2 + s^2B^2\epsilon) + c\sqrt{s}B\epsilon + \Delta_T(\log q, \log q^s). \end{aligned}$$

*Term 3: Estimation error*

We employ 1. Lemma B.2, 2. adding a zero-valued term, 3. triangle inequality, and 4. the definition of our estimator and some linear algebra to obtain

$$\begin{aligned} &\sum_{t=1}^T \mathbb{E}_{X_t, X_{t-1} \sim \mathbb{Q}_{t,t-1}} \left[ \log \frac{p_{t-1|t}^s(X_{t-1}|X_t)}{\hat{p}_{t-1|t}(X_{t-1}|X_t)} \right] \\ &\leq \frac{1-\alpha_t}{2} \sum_{t=1}^T \mathbb{E}_{X_t \sim \mathbb{Q}_t} \|\hat{\kappa} \mathbf{s}_{\hat{\Theta}_{\epsilon_1}}(X_t, t) - \nabla \log q_t^s(X_t)\|^2 \\ &\quad + (1-\alpha_t) \sum_{t=1}^T \sqrt{\mathbb{E}_{X_t \sim \mathbb{Q}_t} \|\nabla \log q_t(X_t) - \nabla \log q_t^s(X_t)\|^2 \mathbb{E}_{X_t \sim \mathbb{Q}_t} \|\nabla \log q_t^s(X_t) - \hat{\kappa} \mathbf{s}_{\hat{\Theta}_{\epsilon_1}}(X_t, t)\|^2} \end{aligned}$$

$$\begin{aligned}
&= \frac{1-\alpha_t}{2} \sum_{t=1}^T \left( \frac{1}{n} \sum_{i=1}^n \|\hat{\kappa} \mathbf{s}_{\hat{\Theta}_{\ell_1}}(\mathbf{x}_t^i, t) - \nabla \log q_t^s(\mathbf{x}_t^i)\|^2 + \mathbb{E}_{X_t \sim Q_t} \|\hat{\kappa} \mathbf{s}_{\hat{\Theta}_{\ell_1}}(X_t, t) - \nabla \log q_t^s(X_t)\|^2 \right. \\
&\quad \left. - \frac{1}{n} \sum_{i=1}^n \|\hat{\kappa} \mathbf{s}_{\hat{\Theta}_{\ell_1}}(\mathbf{x}_t^i, t) - \nabla \log q_t^s(\mathbf{x}_t^i)\|^2 \right) \\
&\quad + (1-\alpha_t) \sum_{t=1}^T \sqrt{\mathbb{E}_{X_t \sim Q_t} \|\nabla \log q_t(X_t) - \nabla \log q_t^s(X_t)\|^2 \mathbb{E}_{X_t \sim Q_t} \|\nabla \log q_t^s(X_t) - \hat{\kappa} \mathbf{s}_{\hat{\Theta}_{\ell_1}}(X_t, t)\|^2} \\
&\leq \frac{1-\alpha_t}{2} \sum_{t=1}^T \left( \frac{1}{n} \sum_{i=1}^n \|\hat{\kappa} \mathbf{s}_{\hat{\Theta}_{\ell_1}}(\mathbf{x}_t^i, t) - \nabla \log q_t(\mathbf{x}_t^i)\|^2 + \frac{1}{n} \sum_{i=1}^n \|\nabla \log q_t(\mathbf{x}_t^i) - \nabla \log q_t^s(\mathbf{x}_t^i)\|^2 \right. \\
&\quad \left. + \mathbb{E}_{X_t \sim Q_t} \|\hat{\kappa} \mathbf{s}_{\hat{\Theta}_{\ell_1}}(X_t, t) - \nabla \log q_t^s(X_t)\|^2 - \frac{1}{n} \sum_{i=1}^n \|\hat{\kappa} \mathbf{s}_{\hat{\Theta}_{\ell_1}}(\mathbf{x}_t^i, t) - \nabla \log q_t^s(\mathbf{x}_t^i)\|^2 \right) \\
&\quad + (1-\alpha_t) \sum_{t=1}^T \sqrt{\mathbb{E}_{X_t \sim Q_t} \|\nabla \log q_t(X_t) - \nabla \log q_t^s(X_t)\|^2 \mathbb{E}_{X_t \sim Q_t} \|\nabla \log q_t^s(X_t) - \hat{\kappa} \mathbf{s}_{\hat{\Theta}_{\ell_1}}(X_t, t)\|^2} \\
&\leq \frac{1-\alpha_t}{2} \sum_{t=1}^T \left( \frac{1}{n} \sum_{i=1}^n \|\kappa \mathbf{s}_{\Theta}(\mathbf{x}_t^i, t) - \nabla \log q_t(\mathbf{x}_t^i)\|^2 + r\kappa^2 - r\hat{\kappa}^2 + \frac{1}{n} \sum_{i=1}^n \|\nabla \log q_t(\mathbf{x}_t^i) - \nabla \log q_t^s(\mathbf{x}_t^i)\|^2 \right. \\
&\quad \left. + \left| \mathbb{E}_{X_t \sim Q_t} \|\hat{\kappa} \mathbf{s}_{\hat{\Theta}_{\ell_1}}(X_t, t) - \nabla \log q_t^s(X_t)\|^2 - \frac{1}{n} \sum_{i=1}^n \|\hat{\kappa} \mathbf{s}_{\hat{\Theta}_{\ell_1}}(\mathbf{x}_t^i, t) - \nabla \log q_t^s(\mathbf{x}_t^i)\|^2 \right| \right) \\
&\quad + (1-\alpha_t) \sum_{t=1}^T \sqrt{\mathbb{E}_{X_t \sim Q_t} \|\nabla \log q_t(X_t) - \nabla \log q_t^s(X_t)\|^2 \mathbb{E}_{X_t \sim Q_t} \|\nabla \log q_t^s(X_t) - \hat{\kappa} \mathbf{s}_{\hat{\Theta}_{\ell_1}}(X_t, t)\|^2}
\end{aligned}$$

for arbitrary function  $\mathbf{s}_{\Theta}(\cdot, \cdot)$  with  $\Theta \in \mathcal{B}_1$  and  $\kappa \in (0, \infty)$ .

Now, by collecting all the pieces of the proof we obtain

$$\begin{aligned}
\text{KL}(\mathbb{Q}_0 \|\hat{P}_0) &\leq c \frac{M}{T^2} + \frac{c}{T} (sB^2 + s^2B^2 + s^2B^2\epsilon) + c\sqrt{s}B\epsilon + \Delta_T(\log q, \log q^s) \\
&\quad + \frac{1-\alpha_t}{2} \sum_{t=1}^T \left( \frac{1}{n} \sum_{i=1}^n \|\kappa \mathbf{s}_{\Theta}(\mathbf{x}_t^i, t) - \nabla \log q_t(\mathbf{x}_t^i)\|^2 + r\kappa^2 - r\hat{\kappa}^2 \right. \\
&\quad \left. + \frac{1}{n} \sum_{i=1}^n \|\nabla \log q_t(\mathbf{x}_t^i) - \nabla \log q_t^s(\mathbf{x}_t^i)\|^2 \right. \\
&\quad \left. + \sup_{\Theta \in \mathcal{B}_1} \left| \mathbb{E}_{X_t \sim Q_t} \|\hat{\kappa} \mathbf{s}_{\Theta}(X_t, t) - \nabla \log q_t^s(X_t)\|^2 - \frac{1}{n} \sum_{i=1}^n \|\hat{\kappa} \mathbf{s}_{\Theta}(\mathbf{x}_t^i, t) - \nabla \log q_t^s(\mathbf{x}_t^i)\|^2 \right| \right. \\
&\quad \left. + 2 \sqrt{\mathbb{E}_{X_t \sim Q_t} \|\nabla \log q_t(X_t) - \nabla \log q_t^s(X_t)\|^2 \mathbb{E}_{X_t \sim Q_t} \|\nabla \log q_t^s(X_t) - \hat{\kappa} \mathbf{s}_{\hat{\Theta}_{\ell_1}}(X_t, t)\|^2} \right).
\end{aligned}$$

A high level idea now is choosing the tuning parameter  $r$  in such a way that the term  $-r\hat{\kappa}^2$  can dominate the terms in the absolute value that are dependent over  $\hat{\kappa}$ . The point here is that the terms in the absolute value are growing in the sparse function space. Employing Lemma 4.2, we obtain for  $r \geq 8\sqrt{2} \log n/n$

$$\begin{aligned}
\text{KL}(\mathbb{Q}_0 \|\hat{P}_0) &\leq \frac{cM}{T^2} + \frac{c}{T} (sB^2 + s^2B^2 + s^2B^2\epsilon) + c\sqrt{s}B\epsilon + \Delta_T(\log q, \log q^s) \\
&\quad + \frac{1-\alpha_t}{2} \sum_{t=1}^T \left( \inf_{\Theta \in \mathcal{B}_1; \kappa \in (0, \infty)} \left\{ \frac{1}{n} \sum_{i=1}^n \|\kappa \mathbf{s}_{\Theta}(\mathbf{x}_t^i, t) - \nabla \log q_t(\mathbf{x}_t^i)\|^2 + r\kappa^2 \right\} \right. \\
&\quad \left. + \frac{1}{n} \sum_{i=1}^n \|\nabla \log q_t(\mathbf{x}_t^i) - \nabla \log q_t^s(\mathbf{x}_t^i)\|^2 + sB^2 \frac{\sqrt{2} \log n}{n} \right)
\end{aligned}$$

$$+ 2\sqrt{\mathbb{E}_{X_t \sim Q_t} \|\nabla \log q_t(X_t) - \nabla \log q_t^s(X_t)\|^2 \mathbb{E}_{X_t \sim Q_t} \|\nabla \log q_t^s(X_t) - \hat{\kappa} \mathbf{s}_{\hat{\Theta}_{\ell_1}}(X_t, t)\|^2}$$

with probability at least  $1 - 32/n^2$ .

Using Assumption 3.3, (4), and (2) we also obtain

$$\begin{aligned} (1 - \alpha_t) \sum_{t=1}^T & \sqrt{\mathbb{E}_{X_t \sim Q_t} \|\nabla \log q_t(X_t) - \nabla \log q_t^s(X_t)\|^2 \mathbb{E}_{X_t \sim Q_t} \|\nabla \log q_t^s(X_t) - \hat{\kappa} \mathbf{s}_{\hat{\Theta}_{\ell_1}}(X_t, t)\|^2} \\ & \leq (1 - \alpha_t) \left( \max_{t \in \{1, \dots, T\}} \sqrt{\mathbb{E}_{X_t \sim Q_t} \|\nabla \log q_t^s(X_t) - \hat{\kappa} \mathbf{s}_{\hat{\Theta}_{\ell_1}}(X_t, t)\|^2} \right) \\ & \quad \sum_{t=1}^T \sqrt{\mathbb{E}_{X_t \sim Q_t} \|\nabla \log q_t(X_t) - \nabla \log q_t^s(X_t)\|^2} \\ & \leq c(\hat{\kappa} + \sqrt{s}B)\epsilon \\ & \leq c\epsilon\sqrt{s}B \\ & \leq c\sqrt{s}B \frac{1}{T}. \end{aligned}$$

Let's note that for the third inequality above we can follow the same approach as in Taheri et al. (2021, Page 155) to conclude that for large enough tuning (just double it),  $\hat{\kappa} \leq 3\kappa^*$  (where  $\kappa^* = \|\nabla \log q_t^s(X_t)\|_\infty \approx B$ ) that gives us the space to remove  $\hat{\kappa}$  from our bounds. Let's also note that under the Assumption 3.3 and (4), we can also conclude that

$$(1 - \alpha_t) \sum_{t=1}^T \frac{1}{n} \sum_{i=1}^n \|\nabla \log q_t(\mathbf{x}_t^i) - \nabla \log q_t^s(\mathbf{x}_t^i)\|^2 \lesssim \epsilon \leq \frac{1}{T}.$$

Finally, collecting displays above, some simplifications, and keeping the dominant factors gives us the desired results.  $\square$

### B.3. Proof of Lemma 4.1

*Proof.* We start the proof with Lemma B.1 that relates  $q_{t-1|t}(\mathbf{x}_{t-1}|\mathbf{x}_t)$  and  $p_{t-1|t}^s(\mathbf{x}_{t-1}|\mathbf{x}_t)$  by

$$q_{t-1|t}(\mathbf{x}_{t-1}|\mathbf{x}_t) \propto p_{t-1|t}^s(\mathbf{x}_{t-1}|\mathbf{x}_t) \exp(\zeta_{t,t-1}(\mathbf{x}_t, \mathbf{x}_{t-1})) \quad (8)$$

with  $\zeta_{t,t-1}(\mathbf{x}_t, \mathbf{x}_{t-1}) = \log q_{t-1}(\mathbf{x}_{t-1}) - \sqrt{\alpha_t} \mathbf{x}_{t-1}^T \nabla \log q_t^s(\mathbf{x}_t) + f(\mathbf{x}_t)$ , where  $f(\mathbf{x}_t)$  is an arbitrary function of  $\mathbf{x}_t$ . Now, let's progress with adding a zero-valued term to the  $\zeta_{t,t-1}(\mathbf{x}_t, \mathbf{x}_{t-1})$

$$\begin{aligned} \zeta_{t,t-1}(\mathbf{x}_t, \mathbf{x}_{t-1}) &= \log q_{t-1}^s(\mathbf{x}_{t-1}) - \sqrt{\alpha_t} \mathbf{x}_{t-1}^T \nabla \log q_t^s(\mathbf{x}_t) \\ & \quad + \log q_{t-1}(\mathbf{x}_{t-1}) - \log q_{t-1}^s(\mathbf{x}_{t-1}) + f(\mathbf{x}_t) \end{aligned}$$

and set  $f(\mathbf{x}_t) = -\log q_{t-1}^s(\mathbf{u}_t^s) + \sqrt{\alpha_t} (\mathbf{u}_t^s)^T \nabla \log q_t^s(\mathbf{x}_t)$ . Then, we have

$$\begin{aligned} \zeta_{t,t-1}(\mathbf{x}_t, \mathbf{x}_{t-1}) &= \log q_{t-1}^s(\mathbf{x}_{t-1}) - \log q_{t-1}^s(\mathbf{u}_t^s) - (\mathbf{x}_{t-1} - \mathbf{u}_t^s)^T \sqrt{\alpha_t} \nabla \log q_t^s(\mathbf{x}_t) \\ & \quad + \log q_{t-1}(\mathbf{x}_{t-1}) - \log q_{t-1}^s(\mathbf{x}_{t-1}). \end{aligned}$$

For a fixed  $\mathbf{x}_t$ , then we have (the denominator is for normalization reason)

$$q_{t-1|t}(\mathbf{x}_{t-1}|\mathbf{x}_t) = \frac{p_{t-1|t}^s(\mathbf{x}_{t-1}|\mathbf{x}_t) \exp(\zeta_{t,t-1}(\mathbf{x}_t, \mathbf{x}_{t-1}))}{\mathbb{E}_{X_{t-1} \sim P_{t-1|t}^s} [\exp(\zeta_{t,t-1}(\mathbf{x}_t, X_{t-1}))]}.$$



We then use the above display and Jensen's inequality to obtain

$$\begin{aligned}
& \mathbb{E}_{X_t, X_{t-1} \sim \mathbb{Q}_{t,t-1}} \left[ \log \frac{q_{t-1|t}(X_{t-1}|X_t)}{p_{t-1|t}^s(X_{t-1}|X_t)} \right] \\
&= \mathbb{E}_{X_t, X_{t-1} \sim \mathbb{Q}_{t,t-1}} \left[ \zeta_{t,t-1}(X_t, X_{t-1}) - \log \mathbb{E}_{X_{t-1} \sim P_{t-1|t}^s} [\exp(\zeta_{t,t-1}(X_t, X_{t-1}))] \right] \\
&= \mathbb{E}_{X_t, X_{t-1} \sim \mathbb{Q}_{t,t-1}} [\zeta_{t,t-1}(X_t, X_{t-1})] - \mathbb{E}_{X_t \sim \mathbb{Q}_t} \left[ \log \mathbb{E}_{X_{t-1} \sim P_{t-1|t}^s} [\exp(\zeta_{t,t-1}(X_t, X_{t-1}))] \right] \\
&\leq \mathbb{E}_{X_t, X_{t-1} \sim \mathbb{Q}_{t,t-1}} [\zeta_{t,t-1}(X_t, X_{t-1})] - \mathbb{E}_{X_t \sim \mathbb{Q}_t} \left[ \mathbb{E}_{X_{t-1} \sim P_{t-1|t}^s} [\zeta_{t,t-1}(X_t, X_{t-1})] \right].
\end{aligned}$$

Now, let's rewrite

$$\begin{aligned}
\zeta_{t,t-1}(\mathbf{x}_t, \mathbf{x}_{t-1}) &= \log q_{t-1}^s(\mathbf{x}_{t-1}) - \log q_{t-1}^s(\mathbf{u}_t^s) - (\mathbf{x}_{t-1} - \mathbf{u}_t^s)^T \sqrt{\alpha_t} \nabla \log q_t^s(\mathbf{x}_t) \\
&\quad + \log q_{t-1}(\mathbf{x}_{t-1}) - \log q_{t-1}^s(\mathbf{x}_{t-1}) \\
&=: \zeta'_{t,t-1}(\mathbf{x}_t, \mathbf{x}_{t-1}) + \log q_{t-1}(\mathbf{x}_{t-1}) - \log q_{t-1}^s(\mathbf{x}_{t-1}).
\end{aligned}$$

We are now left with three terms: 1.  $\mathbb{E}_{X_t, X_{t-1} \sim \mathbb{Q}_{t,t-1}} [\zeta'_{t,t-1}(X_t, X_{t-1})]$ , 2.  $\mathbb{E}_{X_t \sim \mathbb{Q}_t, X_{t-1} \sim P_{t-1|t}^s} [\zeta'_{t,t-1}(X_t, X_{t-1})]$ , and 3.  $\mathbb{E}_{X_t \sim \mathbb{Q}_t} [\mathbb{E}_{X_{t-1} \sim \mathbb{Q}_{t-1|t}} [\log q_{t-1}(X_{t-1}) - \log q_{t-1}^s(X_{t-1})] - \mathbb{E}_{X_{t-1} \sim P_{t-1|t}^s} [\log q_{t-1}(X_{t-1}) - \log q_{t-1}^s(X_{t-1})]]$  and we need to study 1. and 2. in details:

*Term 1:*  $\mathbb{E}_{X_t \sim \mathbb{Q}_t, X_{t-1} \sim P_{t-1|t}^s} [\zeta'_{t,t-1}(X_t, X_{t-1})]$

We 1. use the definition of  $\zeta'_{t,t-1}(X_t, X_{t-1})$ , 2. (Second order) Taylor expand  $\log q_{t-1}^s(X_{t-1})$  around  $\mathbf{u}_t^s$ , 3. use [Liang et al. \(2024, Lemma 7\)](#) that implies  $\mathbb{E}_{X_{t-1} \sim P_{t-1|t}^s} [(X_{t-1}^i - (\mathbf{u}_t^s)^i)^p] = 0 \ \forall p \geq 1 \text{ odd}$  (we use the notation  $X_t^i$  to referenc to the  $i$ th feature of the vector  $X_t$ ), 4. using the fact that  $X_{t-1}^i$  is conditionally independent of  $X_{t-1}^j$  for  $i \neq j$  and again  $\mathbb{E}_{X_{t-1} \sim P_{t-1|t}^s} [(X_{t-1}^i - (\mathbf{u}_t^s)^i)^p] = 0 \ \forall p \geq 1 \text{ odd}$ , and 5.  $\mathbb{E}_{X_{t-1} \sim P_{t-1|t}^s} [(X_{t-1}^i - (\mathbf{u}_t^s)^i)^2] = (1 - \alpha_t)/\alpha_t$  (see (7))

$$\begin{aligned}
& \mathbb{E}_{X_t \sim \mathbb{Q}_t, X_{t-1} \sim P_{t-1|t}^s} [\zeta'_{t,t-1}(X_t, X_{t-1})] \\
&= \mathbb{E}_{X_t \sim \mathbb{Q}_t, X_{t-1} \sim P_{t-1|t}^s} [\log q_{t-1}^s(X_{t-1}) - \log q_{t-1}^s(\mathbf{u}_t^s) - (X_{t-1} - \mathbf{u}_t^s)^T \sqrt{\alpha_t} \nabla \log q_t^s(X_t)] \\
&\approx \mathbb{E}_{X_t \sim \mathbb{Q}_t, X_{t-1} \sim P_{t-1|t}^s} \left[ \nabla \log q_{t-1}^s(\mathbf{u}_t^s)(X_{t-1} - \mathbf{u}_t^s) - (X_{t-1} - \mathbf{u}_t^s)^T \sqrt{\alpha_t} \nabla \log q_t^s(X_t) \right. \\
&\quad \left. + \frac{1}{2} (X_{t-1} - \mathbf{u}_t^s)^T \nabla^2 \log q_{t-1}^s(\mathbf{u}_t^s)(X_{t-1} - \mathbf{u}_t^s) \right] \\
&= \mathbb{E}_{X_t \sim \mathbb{Q}_t, X_{t-1} \sim P_{t-1|t}^s} \left[ \frac{1}{2} (X_{t-1} - \mathbf{u}_t^s)^T \nabla^2 \log q_{t-1}^s(\mathbf{u}_t^s)(X_{t-1} - \mathbf{u}_t^s) \right] \\
&= \frac{1}{2} \sum_{i=1}^d \mathbb{E}_{X_t \sim \mathbb{Q}_t} [(\nabla^2 \log q_{t-1}^s(\mathbf{u}_t^s))_{ii} \mathbb{E}_{X_{t-1} \sim P_{t-1|t}^s} (X_{t-1}^i - (\mathbf{u}_t^s)^i)^2] \\
&= \frac{(1 - \alpha_t)}{2\alpha_t} \sum_{i=1}^d \mathbb{E}_{X_t \sim \mathbb{Q}_t} [(\nabla^2 \log q_{t-1}^s(\mathbf{u}_t^s))_{ii}].
\end{aligned}$$

Note that here (as well as for the Term 2), for keeping the proofs simple and tractable, we use a second-order Taylor expansion and employ the notation  $\approx$ . However, higher-order expansions can also be applied without affecting the dominant rates. As we extend to higher-order Taylor expansions, the dominant factor remains  $O((1 - \alpha_t)/\alpha_t)^2$ , so we omit those terms for simplicity.

*Term 2:*  $\mathbb{E}_{X_t, X_{t-1} \sim \mathbb{Q}_{t,t-1}} [\zeta'_{t,t-1}(X_t, X_{t-1})]$

Following the same approach as in previous step and some further linear algebra we obtain

$$\begin{aligned}
& \mathbb{E}_{X_t, X_{t-1} \sim \mathbb{Q}_{t,t-1}} [\zeta'_{t,t-1}(X_t, X_{t-1})] \\
&= \mathbb{E}_{X_t, X_{t-1} \sim \mathbb{Q}_{t,t-1}} [\log q_{t-1}^s(X_{t-1}) - \log q_{t-1}^s(\mathbf{u}_t^s) - (X_{t-1} - \mathbf{u}_t^s)^T \sqrt{\alpha_t} \nabla \log q_t^s(X_t)] \\
&\approx \mathbb{E}_{X_t, X_{t-1} \sim \mathbb{Q}_{t,t-1}} \left[ \nabla \log q_{t-1}^s(\mathbf{u}_t^s)(X_{t-1} - \mathbf{u}_t^s) - (X_{t-1} - \mathbf{u}_t^s)^T \sqrt{\alpha_t} \nabla \log q_t^s(X_t) \right. \\
&\quad \left. + \frac{1}{2} (X_{t-1} - \mathbf{u}_t^s)^T \nabla^2 \log q_{t-1}^s(\mathbf{u}_t^s)(X_{t-1} - \mathbf{u}_t^s) \right] \\
&= (1 - \sqrt{\alpha_t}) \mathbb{E}_{X_t \sim \mathbb{Q}_t} [\nabla \log q_{t-1}^s(\mathbf{u}_t^s) \mathbb{E}_{X_{t-1} \sim \mathbb{Q}_{t-1|t}} [(X_{t-1} - \mathbf{u}_t^s)]] \\
&\quad + \frac{1}{2} \mathbb{E}_{X_t, X_{t-1} \sim \mathbb{Q}_{t,t-1}} [(X_{t-1} - \mathbf{u}_t^s)^T \nabla^2 \log q_{t-1}^s(\mathbf{u}_t^s)(X_{t-1} - \mathbf{u}_t^s)].
\end{aligned}$$

Employing Liang et al. (2024, Lemma 8; first claim), we have  $\mathbb{E}_{X_{t-1} \sim \mathbb{Q}_{t-1|t}} [X_{t-1}] = \mathbf{u}_t$ . That implies

$$\begin{aligned}
\mathbb{E}_{X_{t-1} \sim \mathbb{Q}_{t-1|t}} [(X_{t-1} - \mathbf{u}_t^s)] &= \mathbb{E}_{X_{t-1} \sim \mathbb{Q}_{t-1|t}} [X_{t-1}] - \mathbf{u}_t^s \\
&= \mathbf{u}_t - \frac{1}{\sqrt{\alpha_t}} (\mathbf{x}_t + (1 - \alpha_t) \nabla \log q_t^s(\mathbf{x}_t)) \\
&= \frac{(1 - \alpha_t)}{\sqrt{\alpha_t}} (\nabla \log q_t(\mathbf{x}_t) - \nabla \log q_t^s(\mathbf{x}_t)).
\end{aligned}$$

Collecting the pieces above together with Cauchy–Schwarz inequality we obtain

$$\begin{aligned}
& \mathbb{E}_{X_t, X_{t-1} \sim \mathbb{Q}_{t,t-1}} [\zeta'_{t,t-1}(X_t, X_{t-1})] \\
&\leq \frac{(1 - \alpha_t)}{\sqrt{\alpha_t}} (1 - \sqrt{\alpha_t}) \sqrt{\mathbb{E}_{X_t \sim \mathbb{Q}_t} \|\nabla \log q_{t-1}^s(\mathbf{u}_t^s)\|^2 \mathbb{E}_{X_t \sim \mathbb{Q}_t} \|\nabla \log q_t(X_t) - \nabla \log q_t^s(X_t)\|^2} \\
&\quad + \frac{1}{2} \mathbb{E}_{X_t, X_{t-1} \sim \mathbb{Q}_{t,t-1}} [(X_{t-1} - \mathbf{u}_t^s)^T \nabla^2 \log q_{t-1}^s(\mathbf{u}_t^s)(X_{t-1} - \mathbf{u}_t^s)].
\end{aligned}$$

Now let's treat the second term in the inequality above by 1. adding a zero-valued term, 2. expanding the product, 3. using Liang et al. (2024, Lemma 8; second claim) and the fact that terms two and three goes to zero and some rewriting

$$\begin{aligned}
& \mathbb{E}_{X_t \sim \mathbb{Q}_t} [\mathbb{E}_{X_{t-1} \sim \mathbb{Q}_{t-1|t}} [(X_{t-1} - \mathbf{u}_t + \mathbf{u}_t - \mathbf{u}_t^s)^T (X_{t-1} - \mathbf{u}_t + \mathbf{u}_t - \mathbf{u}_t^s)]] \\
&= \mathbb{E}_{X_t \sim \mathbb{Q}_t} [\mathbb{E}_{X_{t-1} \sim \mathbb{Q}_{t-1|t}} [(X_{t-1} - \mathbf{u}_t)^T (X_{t-1} - \mathbf{u}_t)]] \\
&\quad + \mathbb{E}_{X_t \sim \mathbb{Q}_t} [\mathbb{E}_{X_{t-1} \sim \mathbb{Q}_{t-1|t}} [(X_{t-1} - \mathbf{u}_t)^T (\mathbf{u}_t - \mathbf{u}_t^s)]] \\
&\quad + \mathbb{E}_{X_t \sim \mathbb{Q}_t} [\mathbb{E}_{X_{t-1} \sim \mathbb{Q}_{t-1|t}} [(\mathbf{u}_t - \mathbf{u}_t^s)^T (X_{t-1} - \mathbf{u}_t)]] \\
&\quad + \mathbb{E}_{X_t \sim \mathbb{Q}_t} [\mathbb{E}_{X_{t-1} \sim \mathbb{Q}_{t-1|t}} [(\mathbf{u}_t - \mathbf{u}_t^s)^T (\mathbf{u}_t - \mathbf{u}_t^s)]] \\
&= \mathbb{E}_{X_t \sim \mathbb{Q}_t} \left[ \frac{1 - \alpha_t}{\alpha_t} \mathbb{I}_d + \frac{(1 - \alpha_t)^2}{\alpha_t} \nabla^2 \log q_t(X_t) \right] \\
&\quad + \mathbb{E}_{X_t \sim \mathbb{Q}_t} \left[ \frac{(1 - \alpha_t)^2}{\alpha_t} (\nabla \log q_t^s(X_t) - \nabla \log q_t(X_t))^T (\nabla \log q_t^s(X_t) - \nabla \log q_t(X_t)) \right]. \tag{9}
\end{aligned}$$

Above results state that our term involving  $(1 - \alpha_t) \mathbb{I}_d / \alpha_t$  can be canceled out by the terms from Step 1. We then need to study the remaining terms that all involve the nice factor  $(1 - \alpha_t)^2$ .

So, collecting all the pieces of the proof, we 1. use the results from Term 1. and Term 2., 2. implying some linear algebra to expand the product, 3. use (9) and cancel out terms involving the multiple  $(1 - \alpha_t)$  (for simplicity we have ignored the last term in (9) since it has a minor affect on our final rates), 4. using our Assumption (3.3),  $\mathbb{E}_{X_t \sim \mathbb{Q}_t} \|\nabla \log q_{t-1}^s(\mathbf{u}_t^s)\|^2 \leq s \|\nabla \log q_{t-1}^s(\mathbf{u}_t^s)\|_\infty^2 \lesssim sB^2$ , 5. once again use the Assumption (3.3) that implies  $s$  sparsity between entries of  $\nabla \log q_{t-1}^s(\mathbf{u}_t^s)$ , that also implies sparsity for the second order derivative (it causes that just a fraction of

entries get involved in those sums) (also note that the last term is appeared regarding the term that we neglected in (9)), and 6. use our Assumption over the step sizes (4) to obtain

$$\begin{aligned}
& \sum_{t=1}^T \mathbb{E}_{X_t, X_{t-1} \sim \mathbb{Q}_{t,t-1}} \left[ \log \frac{q_{t-1|t}(X_{t-1}|X_t)}{p_{t-1|t}^s(X_{t-1}|X_t)} \right] \\
& \leq \sum_{t=1}^T \left( \frac{(1-\alpha_t)}{\sqrt{\alpha_t}} (1-\sqrt{\alpha_t}) \sqrt{\mathbb{E}_{X_t \sim \mathbb{Q}_t} \|\nabla \log q_{t-1}^s(\mathbf{u}_t^s)\|^2 \mathbb{E}_{X_t \sim \mathbb{Q}_t} \|\nabla \log q_t(X_t) - \nabla \log q_t^s(X_t)\|^2} \right. \\
& \quad + \frac{1}{2} \mathbb{E}_{X_t, X_{t-1} \sim \mathbb{Q}_{t,t-1}} \left[ (X_{t-1} - \mathbf{u}_t^s)^T \nabla^2 \log q_{t-1}^s(\mathbf{u}_t^s) (X_{t-1} - \mathbf{u}_t^s) \right] \\
& \quad - \frac{1}{2} \sum_{i=1}^d \mathbb{E}_{X_t \sim \mathbb{Q}_t} (\nabla^2 \log q_{t-1}^s(\mathbf{u}_t^s))_{ii} \left( \frac{1-\alpha_t}{\alpha_t} \right) \Big) \\
& \quad + \sum_{t=1}^T (\mathbb{E}_{X_t \sim \mathbb{Q}_t} [\mathbb{E}_{X_{t-1} \sim \mathbb{Q}_{t-1|t}} [\log q_{t-1}(X_{t-1}) - \log q_{t-1}^s(X_{t-1})]] \\
& \quad - \mathbb{E}_{X_{t-1} \sim P_{t-1|t}^s} [\log q_{t-1}(X_{t-1}) - \log q_{t-1}^s(X_{t-1})]) \\
& \leq \sum_{t=1}^T \left( \frac{(1-\alpha_t)}{\sqrt{\alpha_t}} (1-\sqrt{\alpha_t}) \sqrt{\mathbb{E}_{X_t \sim \mathbb{Q}_t} \|\nabla \log q_{t-1}^s(\mathbf{u}_t^s)\|^2 \mathbb{E}_{X_t \sim \mathbb{Q}_t} \|\nabla \log q_t(X_t) - \nabla \log q_t^s(X_t)\|^2} \right. \\
& \quad + \frac{1}{2} \mathbb{E}_{X_t, X_{t-1} \sim \mathbb{Q}_{t,t-1}} \left[ \sum_{i=1}^d (X_{t-1} - \mathbf{u}_t^s)_i^2 (\nabla^2 \log q_{t-1}^s(\mathbf{u}_t^s))_{ii} \right. \\
& \quad + \sum_{i=1}^d \sum_{j=1, j \neq i}^d (X_{t-1} - \mathbf{u}_t^s)_i (X_{t-1} - \mathbf{u}_t^s)_j (\nabla^2 \log q_{t-1}^s(\mathbf{u}_t^s))_{ij} \Big] \\
& \quad - \frac{1}{2} \sum_{i=1}^d \mathbb{E}_{X_t \sim \mathbb{Q}_t} (\nabla^2 \log q_{t-1}^s(\mathbf{u}_t^s))_{ii} \left( \frac{1-\alpha_t}{\alpha_t} \right) \Big) \\
& \quad + \sum_{t=1}^T (\mathbb{E}_{X_t \sim \mathbb{Q}_t} [\mathbb{E}_{X_{t-1} \sim \mathbb{Q}_{t-1|t}} [\log q_{t-1}(X_{t-1}) - \log q_{t-1}^s(X_{t-1})]] \\
& \quad - \mathbb{E}_{X_{t-1} \sim P_{t-1|t}^s} [\log q_{t-1}(X_{t-1}) - \log q_{t-1}^s(X_{t-1})]) \\
& \leq \sum_{t=1}^T \left( \frac{(1-\alpha_t)}{\sqrt{\alpha_t}} (1-\sqrt{\alpha_t}) \sqrt{\mathbb{E}_{X_t \sim \mathbb{Q}_t} \|\nabla \log q_{t-1}^s(\mathbf{u}_t^s)\|^2 \mathbb{E}_{X_t \sim \mathbb{Q}_t} \|\nabla \log q_t(X_t) - \nabla \log q_t^s(X_t)\|^2} \right. \\
& \quad + \frac{1}{2} \mathbb{E}_{X_t, X_{t-1} \sim \mathbb{Q}_{t,t-1}} \left[ \sum_{i=1}^d \frac{(1-\alpha_t)^2}{\alpha_t} (\nabla^2 \log q_t(X_t))_{ii} (\nabla^2 \log q_{t-1}^s(\mathbf{u}_t^s))_{ii} \right. \\
& \quad + \sum_{i=1}^d \sum_{j=1, j \neq i}^d \frac{(1-\alpha_t)^2}{\alpha_t} (\nabla^2 \log q_t(X_t))_{ij} (\nabla^2 \log q_{t-1}^s(\mathbf{u}_t^s))_{ij} \Big] \Big) \\
& \quad + \sum_{t=1}^T (\mathbb{E}_{X_t \sim \mathbb{Q}_t} [\mathbb{E}_{X_{t-1} \sim \mathbb{Q}_{t-1|t}} [\log q_{t-1}(X_{t-1}) - \log q_{t-1}^s(X_{t-1})]] \\
& \quad - \mathbb{E}_{X_{t-1} \sim P_{t-1|t}^s} [\log q_{t-1}(X_{t-1}) - \log q_{t-1}^s(X_{t-1})]) \\
& \leq \sum_{t=1}^T \left( \frac{(1-\alpha_t)}{\sqrt{\alpha_t}} (1-\sqrt{\alpha_t}) \sqrt{sB^2 \mathbb{E}_{X_t \sim \mathbb{Q}_t} \|\nabla \log q_t(X_t) - \nabla \log q_t^s(X_t)\|^2} \right. \\
& \quad + \frac{1}{2} \mathbb{E}_{X_t, X_{t-1} \sim \mathbb{Q}_{t,t-1}} \left[ \sum_{i=1}^d \frac{(1-\alpha_t)^2}{\alpha_t} (\nabla^2 \log q_t(X_t))_{ii} (\nabla^2 \log q_{t-1}^s(\mathbf{u}_t^s))_{ii} \right.
\end{aligned}$$

$$\begin{aligned}
& + \sum_{i=1}^d \sum_{j=1, j \neq i}^d \frac{(1-\alpha_t)^2}{\alpha_t} (\nabla^2 \log q_t(X_t))_{ij} \left( \nabla^2 \log q_{t-1}^s(\mathbf{u}_t^s) \right)_{ij} \Big] \\
& + \sum_{t=1}^T (\mathbb{E}_{X_t \sim Q_t} [\mathbb{E}_{X_{t-1} \sim Q_{t-1}|t} [\log q_{t-1}(X_{t-1}) - \log q_{t-1}^s(X_{t-1})]] \\
& - \mathbb{E}_{X_{t-1} \sim P_{t-1}^s} [\log q_{t-1}(X_{t-1}) - \log q_{t-1}^s(X_{t-1})]) \\
& \leq \sum_{t=1}^T \left( \frac{(1-\alpha_t)}{\sqrt{\alpha_t}} (1-\sqrt{\alpha_t})(c\sqrt{s}B\epsilon) + \frac{(1-\alpha_t)^2}{\alpha_t} (csB^2) + \frac{(1-\alpha_t)^2}{\alpha_t} (cs^2B^2) + \frac{(1-\alpha_t)^2}{\alpha_t} (cs^2B^2\epsilon) \right) \\
& + \sum_{t=1}^T (\mathbb{E}_{X_t \sim Q_t} [\mathbb{E}_{X_{t-1} \sim Q_{t-1}|t} [\log q_{t-1}(X_{t-1}) - \log q_{t-1}^s(X_{t-1})]] \\
& - \mathbb{E}_{X_{t-1} \sim P_{t-1}^s} [\log q_{t-1}(X_{t-1}) - \log q_{t-1}^s(X_{t-1})]) \\
& \leq c\sqrt{s}B\epsilon + \frac{csB^2}{T} + \frac{cs^2B^2}{T} + \frac{cs^2B^2\epsilon}{T} \\
& + \sum_{t=1}^T (\mathbb{E}_{X_t \sim Q_t} [\mathbb{E}_{X_{t-1} \sim Q_{t-1}|t} [\log q_{t-1}(X_{t-1}) - \log q_{t-1}^s(X_{t-1})]] \\
& - \mathbb{E}_{X_{t-1} \sim P_{t-1}^s} [\log q_{t-1}(X_{t-1}) - \log q_{t-1}^s(X_{t-1})]) ,
\end{aligned}$$

as desired. Note that the constant  $c$  is employed for absorbing all constants and it might change from line to line in the proofs.  $\square$

#### B.4. Proof of Lemma 4.2

*Proof.* Our proof approach is based on symmetrization of probabilities and our sparsity assumptions over  $\nabla \log q_t^s(\mathbf{x}_t)$ .

Let's start with the application of symmetrization of probabilities with  $\zeta_i$  for  $i \in \{1, \dots, n\}$  as i.i.d. Rademacher random variables that are independent of the data [van de Geer \(2016, Lemma 16.1\)](#), and employing Contraction principle ([Ledoux and Talagrand, 2013, Theorem 4.4](#)) to obtain

$$\begin{aligned}
& \Pr \left( \sup_{\Theta \in \mathcal{B}_1} \left| \mathbb{E}_{X_t \sim Q_t} \|\hat{\kappa} \mathbf{s}_\Theta(X_t, t) - \nabla \log q_t^s(X_t, t)\|^2 - \frac{1}{n} \sum_{i=1}^n \|\hat{\kappa} \mathbf{s}_\Theta(\mathbf{x}_t^i, t) - \nabla \log q_t^s(\mathbf{x}_t^i)\|^2 \right| \geq 4\mathcal{R} \sqrt{\frac{2t}{n}} \right) \\
& \leq 4 \Pr \left( \sup_{\Theta \in \mathcal{B}_1} \left| \frac{1}{n} \sum_{i=1}^n \zeta_i \|\hat{\kappa} \mathbf{s}_\Theta(\mathbf{x}_t^i, t) - \nabla \log q_t^s(\mathbf{x}_t^i)\|^2 \right| \geq \mathcal{R} \sqrt{\frac{2t}{n}} \right) \\
& \leq 8 \Pr \left( \sup_{\Theta \in \mathcal{B}_1} \left| \frac{1}{n} \sum_{i=1}^n 2\zeta_i (\|\hat{\kappa} \mathbf{s}_\Theta(\mathbf{x}_t^i, t)\|^2 + \|\nabla \log q_t^s(\mathbf{x}_t^i)\|^2) \right| \geq \mathcal{R} \sqrt{\frac{2t}{n}} \right) \\
& \leq 8 \Pr \left( \sup_{\Theta \in \mathcal{B}_1} \left| \frac{1}{n} \sum_{i=1}^n 2\zeta_i (\|\mathbf{s}_\Theta(\mathbf{x}_t^i, t)\|^2) \right| \geq \frac{\mathcal{R}}{2\hat{\kappa}^2} \sqrt{\frac{2t}{n}} =: t' \right) \\
& \quad + 8 \Pr \left( \sup_{\Theta \in \mathcal{B}_1} \left| \frac{1}{n} \sum_{i=1}^n 2\zeta_i (\|\nabla \log q_t^s(\mathbf{x}_t^i)\|^2) \right| \geq \frac{\mathcal{R}}{2} \sqrt{\frac{2t}{n}} =: t'' \right).
\end{aligned}$$

Then, we employ our definition that  $\sup_{\Theta \in \mathcal{B}_1} \|\mathbf{s}_\Theta(\mathbf{x}_t^i, t)\|_1 \leq 1$  that also implies  $\sup_{\Theta \in \mathcal{B}_1} \|\mathbf{s}_\Theta(\mathbf{x}_t^i, t)\|^2 \leq 1$ . This, can reveal that random variables  $z_i = \zeta_i \|\mathbf{s}_\Theta(\mathbf{x}_t^i)\|^2$  are bounded and have zero-mean. So, we can employ Hoeffding's inequality ([Vershynin, 2018, Theorem 2.6.3](#)) (where we used  $K = \max_{i \in \{1, \dots, n\}} \|z_i\|_{\Psi_2} \leq C \|z_i\|_\infty$  and  $\|a\|^2 = 1/n^2$ ). Same can hold for  $y_i = \zeta_i \|\nabla \log q_t^s(\mathbf{x}_t^i)\|^2$ , that is  $y_i = \zeta_i \|\nabla \log q_t^s(\mathbf{x}_t^i)\|^2$  are zero-mean random variables and bounded  $\|\nabla \log q_t^s(\mathbf{x}_t^i)\|^2 \leq s \|\nabla \log q_t^s(\mathbf{x}_t^i)\|_\infty \leq sB^2$ , where we have used Assumption 3.3 and Assumption 3.4 to conclude that  $\|\nabla \log q_t^s(\mathbf{x}_t^i)\|_\infty =: \kappa^* \approx \|\nabla \log q_t(\mathbf{x}_t^i)\|_\infty \leq B$ . Now, we can progress as following

$$\Pr \left( \sup_{\Theta \in \mathcal{B}_1} \left| \mathbb{E}_{X_t \sim Q_t} \|\hat{\kappa} \mathbf{s}_\Theta(X_t, t) - \nabla \log q_t^s(X_t, t)\|^2 - \frac{1}{n} \sum_{i=1}^n \|\hat{\kappa} \mathbf{s}_\Theta(\mathbf{x}_t^i, t) - \nabla \log q_t^s(\mathbf{x}_t^i)\|^2 \right| \geq 4\mathcal{R} \sqrt{\frac{2t}{n}} \right)$$

$$\begin{aligned}
&\leq 8 \Pr\left(\sup_{\Theta \in \mathcal{B}_1} \left| \frac{1}{n} \sum_{i=1}^n \zeta_i (\|\mathbf{s}_t(\mathbf{x}_t^i, t)\|^2) \right| \geq \frac{\mathcal{R}}{4\hat{\kappa}^2} \sqrt{\frac{2t}{n}} =: t' \right) \\
&\quad + 8 \Pr\left(\sup_{\Theta \in \mathcal{B}_1} \left| \frac{1}{n} \sum_{i=1}^n \zeta_i (\|\nabla \log q_t^s(\mathbf{x}_t^i)\|^2) \right| \geq \frac{\mathcal{R}}{4} \sqrt{\frac{2t}{n}} =: t'' \right) \\
&\leq 16 \exp\left(-\frac{nt'^2}{c}\right) + 16 \exp\left(-\frac{nt''^2}{c's^2B^4}\right).
\end{aligned}$$

And

$$\begin{aligned}
\mathcal{R}^2 &\leq \sup_{\Theta \in \mathcal{B}_1} \frac{1}{n} \sum_{i=1}^n \mathbb{E}_{X_t \sim Q_t} \|\hat{\kappa} \mathbf{s}_\Theta(X_t^i, t) - \nabla \log q_t^s(X_t^i)\|^4 \\
&\leq 2(\hat{\kappa}^4 + sB^4).
\end{aligned}$$

That leaves us with

$$\begin{aligned}
&\Pr\left(\sup_{\Theta \in \mathcal{B}_1} \left| \mathbb{E}_{X_t \sim Q_t} \|\hat{\kappa} \mathbf{s}_\Theta(X_t, t) - \nabla \log q_t^s(X_t)\|^2 - \frac{1}{n} \sum_{i=1}^n \|\hat{\kappa} \mathbf{s}_\Theta(\mathbf{x}_t^i) - \nabla \log q_t^s(\mathbf{x}_t^i)\|^2 \right| \right. \\
&\quad \geq 8(\hat{\kappa}^2 + sB^2) \sqrt{\frac{2t}{n}} \\
&\quad \left. \leq 16 \exp\left(-\frac{2t}{c}\right) + 16 \exp\left(-\frac{2t}{c'}\right) \right).
\end{aligned}$$

That gives

$$\begin{aligned}
&\Pr\left(\sup_{\Theta \in \mathcal{B}_1} \left| \mathbb{E}_{X_t \sim Q_t} \|\hat{\kappa} \mathbf{s}_\Theta(X_t, t) - \nabla \log q_t^s(X_t)\|^2 - \frac{1}{n} \sum_{i=1}^n \|\hat{\kappa} \mathbf{s}_\Theta(\mathbf{x}_t^i, t) - \nabla \log q_t^s(\mathbf{x}_t^i)\|^2 \right| \right. \\
&\quad \geq 8(\hat{\kappa}^2 + sB^2) \sqrt{\frac{2t}{n}} \\
&\quad \left. \leq 32 \exp\left(-\frac{2t}{c}\right) \right).
\end{aligned}$$

For  $t = \log(n)$ , we reach

$$\begin{aligned}
&\Pr\left(\sup_{\Theta \in \mathcal{B}_1} \left| \mathbb{E}_{X_t \sim Q_t} \|\hat{\kappa} \mathbf{s}_\Theta(X_t, t) - \nabla \log q_t^s(X_t)\|^2 - \frac{1}{n} \sum_{i=1}^n \|\hat{\kappa} \mathbf{s}_\Theta(\mathbf{x}_t^i, t) - \nabla \log q_t^s(\mathbf{x}_t^i)\|^2 \right| \right. \\
&\quad \geq 8(\hat{\kappa}^2 + sB^2) \sqrt{\frac{2t}{n}} \\
&\quad \leq 32 \exp\left(-\frac{2 \log n}{c}\right) \\
&\quad \lesssim \frac{32}{n^2}.
\end{aligned}$$

□

## B.5. Proof of Lemma B.1

*Proof.* The proof is based on some simple linear algebra and the definition of forward and backward processes.

We 1. use Bayes' rule, 2. consider a fixed  $\mathbf{x}_t$  ( $q_t(\mathbf{x}_t)$  is omitted since  $\mathbf{x}_t$  is fixed), 3. definition of the forward process, and

4. multiplying with a one-valued factor and some rewriting, and 4. and some further rewriting

$$\begin{aligned}
q_{t-1|t}(\mathbf{x}_{t-1}|\mathbf{x}_t) &= \frac{q_{t|t-1}(\mathbf{x}_t|\mathbf{x}_{t-1})q_{t-1}(\mathbf{x}_{t-1})}{q_t(\mathbf{x}_t)} \\
&\propto q_{t|t-1}(\mathbf{x}_t|\mathbf{x}_{t-1})q_{t-1}(\mathbf{x}_{t-1}) \\
&\propto q_{t-1}(\mathbf{x}_{t-1}) \exp\left(-\frac{\|\mathbf{x}_t - \sqrt{\alpha_t}\mathbf{x}_{t-1}\|^2}{2(1-\alpha_t)}\right) \\
&\propto p_{t-1|t}^s(\mathbf{x}_{t-1}|\mathbf{x}_t) \exp\left(\log q_{t-1}(\mathbf{x}_{t-1}) + \frac{\alpha_t\|\mathbf{x}_{t-1} - \mathbf{u}_t^s\|^2}{2(1-\alpha_t)} - \frac{\|\mathbf{x}_t - \sqrt{\alpha_t}\mathbf{x}_{t-1}\|^2}{2(1-\alpha_t)}\right) \\
&= p_{t-1|t}^s(\mathbf{x}_{t-1}|\mathbf{x}_t) \exp\left(\log q_{t-1}(\mathbf{x}_{t-1}) + \frac{\alpha_t\|\mathbf{x}_{t-1} - \mathbf{u}_t^s\|^2}{2(1-\alpha_t)} - \frac{\alpha_t\|\mathbf{x}_{t-1} - (\mathbf{x}_t/\sqrt{\alpha_t})\|^2}{2(1-\alpha_t)}\right)
\end{aligned}$$

using the fact that (see (7))

$$p_{t-1|t}^s(\mathbf{x}_{t-1}|\mathbf{x}_t) \propto \exp\left(-\frac{\alpha_t\|\mathbf{x}_{t-1} - \mathbf{u}_t^s\|^2}{2(1-\alpha_t)}\right).$$

We then use the fact that

$$\begin{aligned}
\|\mathbf{x}_{t-1} - \mathbf{u}_t^s\|^2 - \|\mathbf{x}_{t-1} - (\mathbf{x}_t/\sqrt{\alpha_t})\|^2 &= \|\mathbf{x}_{t-1} - (\mathbf{x}_t/\sqrt{\alpha_t}) + (\mathbf{x}_t/\sqrt{\alpha_t}) - \mathbf{u}_t^s\|^2 - \|\mathbf{x}_{t-1} - (\mathbf{x}_t/\sqrt{\alpha_t})\|^2 \\
&= 2(\mathbf{x}_{t-1} - (\mathbf{x}_t/\sqrt{\alpha_t}))^T ((\mathbf{x}_t/\sqrt{\alpha_t}) - \mathbf{u}_t^s) + \|(\mathbf{x}_t/\sqrt{\alpha_t}) - \mathbf{u}_t^s\|^2.
\end{aligned}$$

We then use (7) to obtain

$$\begin{aligned}
\frac{2(\mathbf{x}_{t-1} - (\mathbf{x}_t/\sqrt{\alpha_t}))^T ((\mathbf{x}_t/\sqrt{\alpha_t}) - \mathbf{u}_t^s)}{(1-\alpha_t)/\alpha_t} &= -(\mathbf{x}_{t-1} - (\mathbf{x}_t/\sqrt{\alpha_t}))^T \sqrt{\alpha_t} \nabla \log q_t^s(\mathbf{x}_t) \\
&= -\sqrt{\alpha_t} \mathbf{x}_{t-1}^T \nabla \log q_t^s(\mathbf{x}_t) + \mathbf{x}_t^T \nabla \log q_t^s(\mathbf{x}_t).
\end{aligned}$$

Collecting all the pieces above we obtain for a fixed  $\mathbf{x}_t$

$$q_{t-1|t}(\mathbf{x}_{t-1}|\mathbf{x}_t) \propto p_{t-1|t}^s(\mathbf{x}_{t-1}|\mathbf{x}_t) \exp(\zeta_{t,t-1}(\mathbf{x}_t, \mathbf{x}_{t-1}))$$

with  $\zeta_{t,t-1}(\mathbf{x}_t, \mathbf{x}_{t-1}) = \log q_{t-1}(\mathbf{x}_{t-1}) - \sqrt{\alpha_t} \mathbf{x}_{t-1}^T \nabla \log q_t^s(\mathbf{x}_t) + f(\mathbf{x}_t)$ , where  $f(\mathbf{x}_t)$  can be considered as an arbitrary function of  $\mathbf{x}_t$ , since  $\mathbf{x}_t$  was fixed (let's also note that the term  $\|(\mathbf{x}_t/\sqrt{\alpha_t}) - \mathbf{u}_t^s\|^2$  is omitted since it is just dependent over  $\mathbf{x}_t$ ). That completes the proof. □

## B.6. Proof of Lemma B.2

*Proof.* We employ the fact that  $\hat{p}$  and  $p^s$  are both Gaussian with the same variance,  $\hat{P}_{t-1|t} = \mathcal{N}(\mathbf{x}_{t-1}; \hat{\mathbf{u}}_t(\mathbf{x}_t), \sigma_t^2 \mathbb{I}_d)$  and  $P_{t-1|t}^s = \mathcal{N}(\mathbf{x}_{t-1}; \mathbf{u}_t^s(\mathbf{x}_t), \sigma_t^2 \mathbb{I}_d)$  with

$$\hat{\mathbf{u}}_t(\mathbf{x}_t) = \frac{1}{\sqrt{\alpha_t}}(\mathbf{x}_t + (1-\alpha_t)\kappa \mathbf{s}_\Theta(\mathbf{x}_t, t))$$

and

$$\mathbf{u}_t^s(\mathbf{x}_t) = \frac{1}{\sqrt{\alpha_t}}(\mathbf{x}_t + (1-\alpha_t)\nabla_{\mathbf{x}_t} \log q_t^s(\mathbf{x}_t)).$$

We use 1.the Gaussian property, 2. rewriting, 3. add a zero-valued term, 4. use the property that  $\mathbb{E}_{X_{t-1} \sim Q_{t-1|t}}[X_{t-1} | \mathbf{x}_t] = \mathbf{u}_t(\mathbf{x}_t)$ , 5. definitions of  $\mathbf{u}_t$ ,  $\mathbf{u}^s$ , and  $\hat{\mathbf{u}}_t$  and Cauchy–Schwarz inequality to obtain

$$\begin{aligned}
& \mathbb{E}_{X_t, X_{t-1} \sim Q_{t,t-1}} \left[ \log \frac{p_{t-1|t}^s(X_{t-1} | X_t)}{\hat{p}_{t-1|t}(X_{t-1} | X_t)} \right] \\
&= \mathbb{E}_{X_t, X_{t-1} \sim Q_{t,t-1}} \left[ \frac{\alpha_t}{2(1-\alpha_t)} (\|X_{t-1} - \hat{\mathbf{u}}_t(X_t)\|^2 - \|X_{t-1} - \mathbf{u}^s(X_t)\|^2) \right] \\
&= \mathbb{E}_{X_t, X_{t-1} \sim Q_{t,t-1}} \left[ \frac{\alpha_t}{(1-\alpha_t)} (X_{t-1} - \mathbf{u}_t^s(X_t))^T (\mathbf{u}_t^s(X_t) - \hat{\mathbf{u}}_t(X_t)) \right. \\
&\quad \left. + \frac{\alpha_t}{2(1-\alpha_t)} \|\mathbf{u}_t^s(X_t) - \hat{\mathbf{u}}_t(X_t)\|^2 \right] \\
&= \mathbb{E}_{X_t, X_{t-1} \sim Q_{t,t-1}} \left[ \frac{\alpha_t}{(1-\alpha_t)} (X_{t-1} - \mathbf{u}_t(X_t) + \mathbf{u}_t(X_t) - \mathbf{u}_t^s(X_t))^T (\mathbf{u}_t^s(X_t) - \hat{\mathbf{u}}_t(X_t)) \right. \\
&\quad \left. + \frac{\alpha_t}{2(1-\alpha_t)} \|\mathbf{u}_t^s(X_t) - \hat{\mathbf{u}}_t(X_t)\|^2 \right] \\
&= \mathbb{E}_{X_t, X_{t-1} \sim Q_{t,t-1}} \left[ \frac{\alpha_t}{(1-\alpha_t)} (\mathbf{u}_t(X_t) - \mathbf{u}_t^s(X_t))^T (\mathbf{u}_t^s(X_t) - \hat{\mathbf{u}}_t(X_t)) \right. \\
&\quad \left. + \frac{\alpha_t}{2(1-\alpha_t)} \|\mathbf{u}_t^s(X_t) - \hat{\mathbf{u}}_t(X_t)\|^2 \right] \\
&\leq (1-\alpha_t) \sqrt{\mathbb{E}_{X_t \sim Q_t} \|\nabla \log q_t(X_t) - \nabla \log q_t^s(X_t)\|^2 \mathbb{E}_{X_t \sim Q_t} \|\nabla \log q_t^s(X_t) - \hat{\kappa} \mathbf{s}_{\hat{\Theta}_{\ell_1}}(X_t, t)\|^2} \\
&\quad + \frac{1-\alpha_t}{2} \mathbb{E}_{X_t \sim Q_t} \|\hat{\kappa} \mathbf{s}_{\hat{\Theta}_{\ell_1}}(X_t, t) - \nabla \log q_t^s(X_t)\|^2.
\end{aligned}$$

That implies

$$\begin{aligned}
& \sum_{t=1}^T \mathbb{E}_{X_t, X_{t-1} \sim Q_{t,t-1}} \left[ \log \frac{p_{t-1|t}^s(X_{t-1} | X_t)}{\hat{p}_{t-1|t}(X_{t-1} | X_t)} \right] \\
&\leq (1-\alpha_t) \sum_{t=1}^T \sqrt{\mathbb{E}_{X_t \sim Q_t} \|\nabla \log q_t(X_t) - \nabla \log q_t^s(X_t)\|^2 \mathbb{E}_{X_t \sim Q_t} \|\nabla \log q_t^s(X_t) - \hat{\kappa} \mathbf{s}_{\hat{\Theta}_{\ell_1}}(X_t, t)\|^2} \\
&\quad + \frac{1-\alpha_t}{2} \sum_{t=1}^T \mathbb{E}_{X_t \sim Q_t} \|\hat{\kappa} \mathbf{s}_{\hat{\Theta}_{\ell_1}}(X_t, t) - \nabla \log q_t^s(X_t)\|^2,
\end{aligned}$$

as desired. □